CALIFORNIA ENERGY COMMISSION

CALIFORNIA NATURAL RESOURCES AGENCY

ENERGY RESEARCH AND DEVELOPMENT DIVISION

FINAL PROJECT REPORT

A Numerical Modeling Framework to Evaluate Effects of Offshore Wind Farms on California's Coastal Upwelling Ecosystem

PREPARED BY:

Kaus Raghukumar, Tim Nelson, and Grace Chang
Integral Consulting Inc.
Chris Chartrand, Lawrence Cheung, and Jesse Roberts
Sandia National Laboratories
Michael Jacox and Jerome Fiechter
University of California, Santa Cruz
Primary Authors

David Stoms, Ph.D.
Project Manager
California Energy Commission
Energy Research and Development Division

Agreement Number: EPC-19-009

Jonah Steinbuck, Ph.D.
Director
ENERGY RESEARCH AND DEVELOPMENT DIVISION

Drew Bohan
Executive Director

ACKNOWLEDGEMENTS

PREFACE

The California Energy Commission's (CEC) Energy Research and Development Division supports energy research and development programs to spur innovation in energy efficiency, renewable energy and advanced clean generation, energy-related environmental protection, energy transmission, and distribution and transportation.

In 2012, the Electric Program Investment Charge (EPIC) was established by the California Public Utilities Commission to fund public investments in research to create and advance new energy solutions, foster regional innovation, and bring ideas from the lab to the marketplace. The EPIC Program is funded by California utility customers under the auspices of the California Public Utilities Commission. The CEC and the state's three largest investor-owned utilities— Pacific Gas and Electric Company, San Diego Gas and Electric Company, and Southern California Edison Company—were selected to administer the EPIC funds and advance novel technologies, tools, and strategies that provide benefits to their electric ratepayers.

The CEC is committed to ensuring public participation in its research and development programs that promote greater reliability, lower costs, and increase safety for the California electric ratepayer and include:

- Providing societal benefits.
- Reducing greenhouse gas emission in the electricity sector at the lowest possible cost.
- Supporting California's loading order to meet energy needs first with energy efficiency and demand response, next with renewable energy (distributed generation and utility scale), and finally with clean, conventional electricity supply.
- Supporting low-emission vehicles and transportation.
- Providing economic development.
- Using ratepayer funds efficiently.

For more information about the Energy Research and Development Division, please visit the CEC's research website (www.energy.ca.gov/research/) or contact the Energy Research and Development Division at ERDD@energy.ca.gov.

ABSTRACT

In California's offshore waters, sustained northwesterly winds are a key energy resource that could contribute substantially to the state's mandated renewable energy goals. However, the development of large-scale offshore windfarms could potentially reduce wind stress at the sea surface, which could then in turn affect wind-driven upwelling, which affects nutrient delivery and ecosystem dynamics. By linking atmospheric and ocean circulation models with simulated wind turbine installation scenarios spread across California wind energy areas of interest, this research concluded that turbines could reduce wind speed downwind of wind farms. This reduction of wind speed would enhance cross-shore changes in wind speeds, leading to reduced upwelling on the inshore side of wind farms and increased upwelling on the offshore side. These changes, when expressed in terms of widely used metrics for upwelling volume transport and nutrient delivery, show that while the net upwelling in a wide coastal band changes relatively little, the spatial structure of upwelling within this coastal region can be shifted outside the bounds of natural variability. Determining how those changes in upwelling patterns might affect the California Current's rich ecosystem requires additional study.

Table of Contents

LIST OF FIGURES

LIST OF TABLES

Executive Summary

Background

To meet California's ambitious clean-energy mandates, rapid advancements are required in energy technology, installed capacity, and new renewable-energy resources. In California's offshore waters, sustained northwesterly winds represent an emerging energy resource. Because wind-energy development is relatively new to the California Coast, there are many knowledge gaps in its potential environmental impacts, both for individual wind-energy facilities and for the cumulative effects of multiple developments. Research is needed to fill these gaps for sustainable development of this clean-energy resource.

The ecological richness of the California coast is a direct result of offshore winds; the wind stress on the sea surface pushes surface waters further offshore, bringing deep, nutrient-rich waters to replace them, a process called *upwelling*. California's wind-driven upwelling of nutrients feeds enormous populations of plankton at the bottom of a robust food chain that includes fish, seabirds, and marine mammals in one of the richest ecosystems on the planet. The California Current, which flows southward along the western coast, contains areas of interest for offshore wind energy. It also supports a commercial and recreational fishing and maritime economy valued at approximately $22 billion. Because wind turbines reduce the energy in a wind field downwind of a facility, wind turbines could potentially adversely affect both local and regional wind-driven upwelling, nutrient delivery, and the entire food chain.

It is therefore essential to investigate the physical effects of large-scale wind facilities on coastal upwelling; the results could then be used to evaluate potential cascading ecosystem and socioeconomic effects. This study improves scientific understanding of a range of effects of wind energy reductions on physical circulation using both historical climate data and future climate projections. These results provide a risk-assessment foundation for the effects of these physical changes in upwelling on organisms at the bottom of the marine food chain, which can impact both ecosystem function and services, including fisheries.

Project Purpose and Approach

The overall goals of this project were to determine potential changes in California's coastal upwelling caused by offshore wind turbines in a variety of environmental conditions, turbine characteristics, and wind farm configurations. Specific objectives included running state-of-the-art models that represent atmosphere and ocean circulation; calculating metrics of the strength of upwelling; and evaluating the sensitivity of upwelling effects to turbine type, geographic regions of deployment, and climate change.

The effects of offshore wind turbines on wind stress fields were studied using a high-resolution atmospheric model that projected alterations to the wind field caused by an array of wind turbines (a wind farm). Atmospheric model results for the baseline (no windfarm) and modi-fied (simulated windfarm) scenarios were then input into an ocean-circulation model of the United States West Coast. Upwelling indices were computed for both baseline and modified

scenarios to estimate changes in upwelling from offshore wind-turbine deployment. Parameters in the modeling system were adjusted to assess sensitive environmental variables, and to consider turbine capacity (10 MW versus 15 MW) and numbers, locations, and configurations of arrays. The environmental variability in the sensitivity analysis included a range of expected wind conditions and offshore circulation that bookend minimum and maximum projected climate-change variabilities over the lifecycle of an offshore wind project.

The locations of the hypothetical wind farms were based on recent offshore wind-energy planning efforts and related studies. The core scenario was based on simulations of wind-energy development in three call areas initially designated by the federal Bureau of Ocean Energy Management in October 2018: Humboldt, Morro Bay, and Diablo Canyon. For the sensitivity analysis, another scenario was studied that included only the Humboldt and Morro Bay wind-energy areas auctioned for lease in December 2022; the Diablo Canyon call area is not under consideration at this time. Lastly, a scenario was included that could achieve a 20-GW capacity with the addition of two areas of interest in Northern California (Del Norte and Cape Mendocino), and larger 15-MW turbines. The first sensitivity analysis therefore represents short-term plans for offshore wind-energy development and the second represents the longer-term trajectory.

Key Results

This study quantified potential effects to upwelling ocean circulation caused by the simulated presence of wind turbines. Key results from this study follow.

- For the core modeling scenario consisting of 10-MW turbines in Humboldt, Morro Bay and Diablo Canyon, wind speeds at 10 m above the sea surface were reduced by approximately 5 percent, with wind farm wakes extending approximately 200 kilometers downwind of offshore wind-energy facilities.

- The introduction of wind turbines showed very little effect within a 10-km coastal band where upwelling is usually the strongest.

- Changes in upwelling outside this 10-km coastal band showed a pronounced cross-shore structure greater than modeled natural variability.

- Net changes to upwelling were modest when spread over a wide 100-km coastal zone.

Knowledge Transfer and Next Steps

To disseminate the results of this research the project team produced and presented the following:

- The team briefed the California Coastal Commission and BOEM in early 2022 to provide project updates on how early data sets could support decision processes.

- A public webinar on the project results was held on June 16, 2022, hosted by the Pacific Ocean Energy Trust. https://www.youtube.com/watch?v=IKs3nKMWoBQ&theme Refresh=1

- A paper on the atmospheric modeling effort was published in *Frontiers in Energy Research* (Raghukumar, K., Chartrand, C., Chang, G., Cheung, L. and Roberts, J., 2022. Effect of Floating Offshore Wind Turbines on Atmospheric Circulation in California. *Frontiers in Energy Research*, p.660.)

- A paper on the ocean-atmosphere modeling was published in *Nature Communications Earth and Environment* (Raghukumar, K., Nelson, T., Jacox, M. et al., projected cross-shore changes in upwelling induced by offshore wind farm development along the California Coast. *Commun Earth Environ* 4, 116 [2023]. https://doi.org/10.1038/s43247-023-00780-y).

Potential avenues of future research include:

- Evaluation of upwelling effects on the food chain such as phytoplankton, zooplankton and krill, and the higher-level organisms that depend on them including fish, seabirds, and marine mammals. The current study projected changes in the physical processes associated with upwelling, but the accurate estimation of ecosystem responses requires additional knowledge of the responses of phytoplankton, zooplankton, and higher trophic-level organisms to physical driving factors, which were beyond the scope of this study.

- Use of a formal risk-assessment framework to evaluate fisheries and related socioeconomic effects.

- Evaluation of mixing and turbulence from wind-turbine structures in the water column and their effects on larger-scale upwelling circulation. The current study only modeled the operation of turbines for converting energy from wind.

- Use of fully-coupled models capable of accounting for the two-way momentum exchange across the air-sea interface. The current study only accounted for changes in the atmosphere that affect ocean circulation. A future study could also account for changes in wave patterns that affect near-surface air flow by changing surface roughness.

CHAPTER 1:
Introduction

In California's offshore waters, sustained northwesterly winds are a key energy resource, with offshore wind resource potential estimated at 112 gigawatts (GW) (Musial et al., 2016). This energy would substantially contribute to California's ambitious renewable resource energy mandates. The California Energy Commission (CEC) was directed by Assembly Bill 525 to establish megawatt planning goals for 2030 and 2045. Governor Gavin Newson asked the CEC to establish an offshore wind planning goal of at least 20 GW by 2045. The CEC ultimately set planning goals of between 2-5 GW for offshore wind in 2030 and 25 GW in 2045 (Flint et al., 2022). The key advantage of offshore wind over its land-based counterpart is that offshore winds are far more consistent and reliable, with few of the topographic and small-scale variables that can plague land-based windfarms. Floating offshore technologies are projected to operate at an average of 70 percent of their maximum power capacity, while the cost of producing that energy could decrease by as much as 53 percent by 2050 from a 2014 baseline (Wiser et al., 2016). However, a lack of understanding of its potential environmental effects is one current barrier to offshore wind farms, which requires further investigation.

Wind-driven upwelling in the California Current is responsible for much of the primary productivity that sustains one of the richest ecosystems on the planet (Xiu et al., 2018). Wind-driven upwelling along the California coast is forced two ways (Figure 1). First, northwesterly winds drive offshore Ekman transport near the coast, which produces both coastal divergence and upwelling of cool, deep, nutrient-rich waters in a band adjacent to the coast, whose width is approximately the baroclinic Rossby radius of deformation (in the range of 10-20 km at these latitudes). Second, wind stress curl (horizontal gradients in the wind) drives divergent flow near the ocean's surface and subsequent upwelling (Ekman suction) that can extend 100-200 km further offshore than that driven by coastal divergence (Rykaczewski and Checkley 2008, Checkley and Barth 2009). In both cases, the occurrence of upwelling is characterized by the upward tilting of constant density surfaces (isopycnals) toward either the coast (coastal upwelling) or toward an upwelling zone (curl-driven upwelling).

Figure 1: Schematic of Upwelling Processes
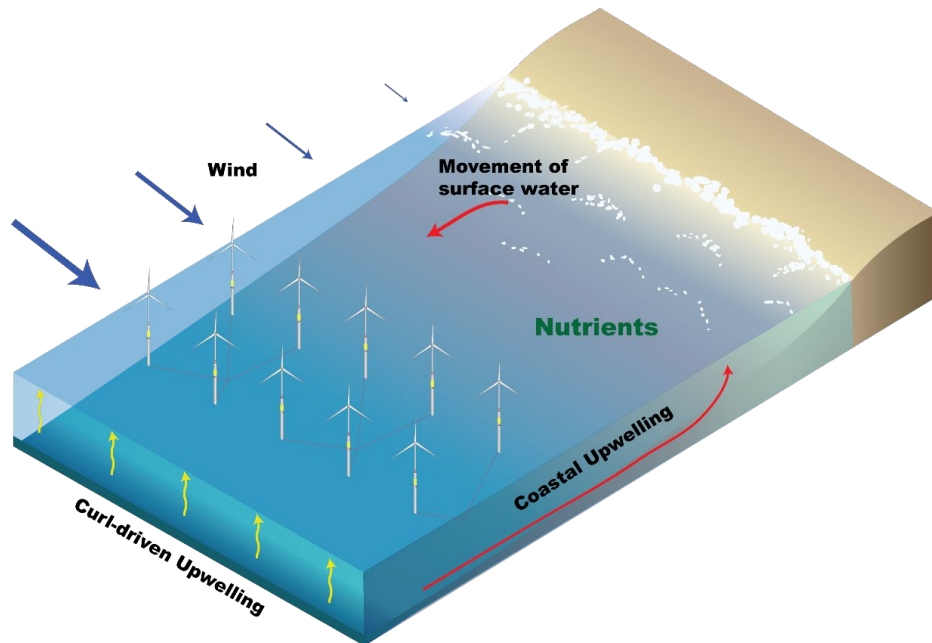
Schematic shows coastal upwelling in a narrow coastal band and curl-driven upwelling over a larger offshore area.

Source: Integral Consulting, Inc.

An offshore wind farm project equal to an approximate lease block area of 20 x 20 km is on the order of spatial scales at which rotational effects such as upwelling occur (Szoeke and Richmand, 1984). The development of offshore wind-energy projects on spatial scales (approaching the baroclinic Rossby radius of deformation) could potentially reduce wind stress at the sea surface and introduce a horizontal shear in wind speeds (wind stress curl), which could have local or regional impacts on California's coastal and curl-driven upwelling, nutrient delivery, and ecosystem dynamics. This study is a first step toward greater understanding of the effects of offshore wind farms on upwelling ecosystems by exploring changes in the physical circulation that could eventually form the basis for an ecosystem risk assessment and socioeconomic analysis.

There are few studies of the effects of large-scale offshore wind turbines on wind-driven upwelling. Wind stress reductions have been examined (Jiménez et al., 2015, Duin, 2019, and Christiansen et al., 2022), however, for a large offshore wind farm in the North Sea. Typical wind speeds of 10 m above the sea surface were reduced by up to 1 m/s, with secondary effects on air temperature, relative humidity, and radiation. In response to changes in wind speed, the formation of wind stress curl-driven upwelling in a large wind farm district also resulted in isopycnal displacement (Broström, 2008), which suggests changes to both down-welling and upwelling, both increased as a function of wind farm lateral extent. Wind farm wakes can increase the magnitude of pycnocline displacements (Paskyabi and Fer, 2012, Paskyabi, 2015), and modulations in the pycnocline displacement can change the spatial-temporal patterns in coastal upwelling. Most recently, the presence of an upwelling/downwelling dipole was measured in the German Bight (indicative of the presence of adjacent upwelling and downwelling regions) and characterized by changes in mixed-layer depth and

potential energy (Floeter et al., 2022). These studies focused on European wind farms, which are often in shallower water than waters off the United States West Coast, and are not specifically located in a region such as the California Current System (CCS), where contributions to wind-driven upwelling include both the wind stress curl and coastal components, both of which can be affected by reducing wind stress.

Three California offshore wind energy areas of interest (Humboldt, Morro Bay, and Diablo Canyon) were originally recognized by the state of California and the Bureau of Ocean Energy Management (BOEM) (Docket No. BOEM-2018- 0045) as regions with suitable offshore wind resources (Musial et al., 2016). These sites in Central and Northern California are biologically and commercially important, providing habitat for multiple endangered species, and supporting a portion of the CCS's commercial and recreational fishing economy, valued at approximately $22 billion (National Marine Fisheries Service [NMFS], 2018).

Specific to California, two atmospheric models have been implemented, one for a hypothetical 10 x 10 km wind farm offshore of Bodega Bay, California (Huang and Hall, 2015) and one for a hypothetical buildout of 877 wind turbines in waters 600-800 m deep offshore of Humboldt, Morro Bay, and Diablo Canyon (this study). Both studies found that wind speeds at 10 m height were reduced by approximately 5 percent, and at full buildout, wakes extended approximately 200 km downwind of wind energy areas of interest. With the length scale of wind-speed reductions on the order of 250 km, the changes reported were estimated on spatial scales large enough to influence upwelling off the West Coast.

In this study, an atmosphere-ocean circulation model evaluated changes to coastal and curl-driven upwelling following introduction of simulated offshore full-wind-energy facilities offshore of Humboldt, Morro Bay, and Diablo Canyon. Wind fields in the presence of wind farms provided the surface forcing fields that, in part, drive ocean circulation (Raghukumar et al., 2022). Since the density of turbines considered here is likely to be near the maximum potential, the results represent an upper boundary on the potential upwelling effects of offshore wind for these three areas of interest.
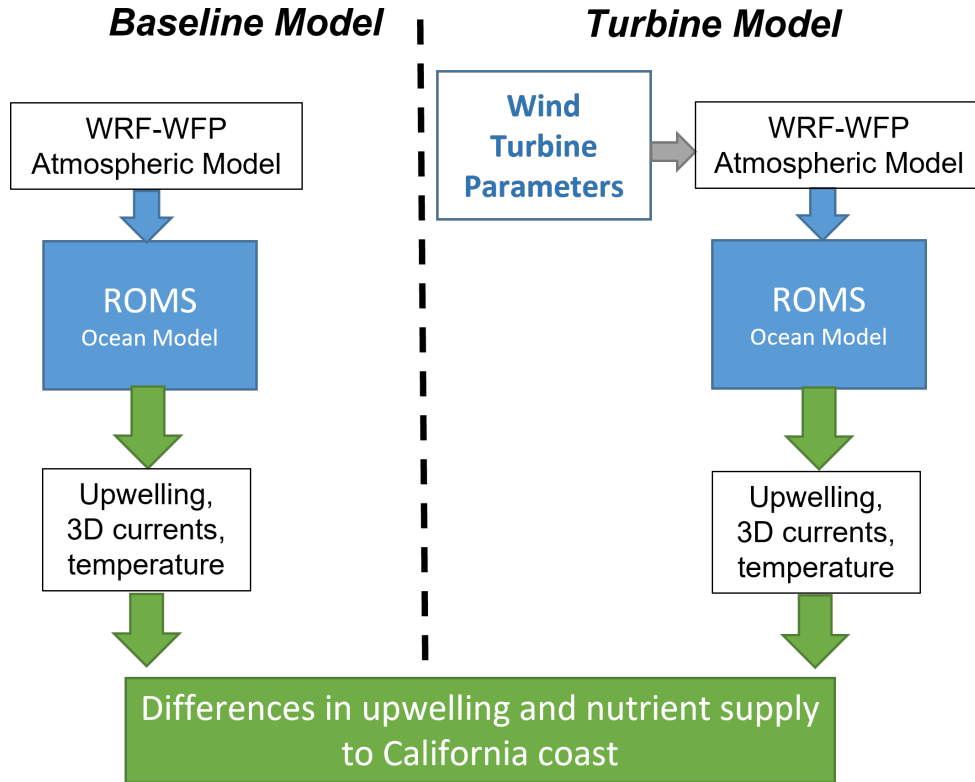
CHAPTER 2:
Project Approach

Advances in high-performance computing allow the application of regional-scale numerical circulation models that provide insight into the various driving forces and sensitivities of upwelling dynamics (Veneziani et al., 2009). This modeling study used a high-resolution atmospheric model, the Weather Research and Forecasting (WRF) model, with wind farm parameterization (WFP) (Fitch et al., 2012), which represents wind turbines as a momentum sink and turbulence source. WRF-WFP uses turbine parameters such as hub height, rotor diameter, power curve, and thrust coefficients to calculate the magnitude of source and sink terms (Lee and Lundquist, 2017). By allowing wind farm parameterization within an established and validated operational weather model, WRF-WFP has been used in a number of studies to evaluate the effects of wind farms on mesoscale weather patterns (Jiménez et al., 2015, Huang and Hall, 2015, Eriksson et al., 2015). The WRF-WFP model accounts for turbine-turbine and wake-turbine interactions, so provides an accurate assessment of the wind field around a wind farm (Churchfield et al., 2012). This WRF-WFP atmospheric model was implemented for the Eastern Pacific, with a higher resolution domain (also called a nest) that contains the continental shelf along the California coast (Raghukumar et al., 2022). Simulated offshore wind turbines were placed within three wind-energy areas of interest, each approximately 100 x 100 km, and located approximately 30 km offshore of Humboldt, Morro Bay, and Diablo Canyon. As of early 2023, the Diablo Canyon area of interest was no longer actively under consideration while the size and shape of the Morro Bay area, including the areas of Morro Bay 399 and Morro Bay 376, were modified by BOEM. The bulk of this study uses the Morro Bay 399 area of interest, along with the existing Humboldt and Diablo Canyon areas of interest. Additional sensitivity studies utilize the Morro Bay 376 area, along with additional areas of interest in Del Norte and Cape Mendocino that were first identified (Collier et al., (2019).

WRF-WFP model wind fields computed in the absence and presence of wind turbines were used to force a regional ocean circulation model (Figure 2), the Regional Ocean Modeling System (ROMS), which also contained a higher resolution grid encompassing the wind farms. While WRF-WRF has been coupled to ocean models in the North Sea (Christiansen et al., 2022), this effort represents the first such effort for the California Coast. This nesting allowed for both the computation of upwelling indices of relevance to primary production and potential changes in these indices (Jacox et al., 2018).

The atmospheric modeling was conducted by project partner Sandia National Laboratories, while the ocean modeling was conducted by Integral Consulting, Inc., (Integral) personnel, with advice from project partners at the University of California, Santa Cruz (UCSC) and the National Ocean and Atmospheric Administration (NOAA). Upwelling metrics were computed by UCSC/NOAA and analyzed jointly with Integral. Regular updates on project progress were provided to the technical advisory committee, comprising of Genevra Harker-Klimĕs, Jaime

Jahncke, Fayçal Kessouri, Sharon Kramer, Chris Potter, Tyler Studds, and Susan Zaleski. Additionally, technical advice was regularly provided by Thomas Kilpatrick and Lisa Gilbane.

Specifics of the modeling approach follow.

Figure 2: Flowchart of Modeling Approach

Baseline Model | *Turbine Model*

WRF-WFP Atmospheric Model

Wind Turbine Parameters → WRF-WFP Atmospheric Model

ROMS
Ocean Model

ROMS
Ocean Model

Upwelling, 3D currents, temperature

Upwelling, 3D currents, temperature

Differences in upwelling and nutrient supply to California coast

Flowchart of modeling approach to evaluate changes to upwelling following the introduction of an offshore wind farm

Source: Integral Consulting, Inc.

Atmospheric Model

The WRF-WFP model (Skamarock et al., 2019) was used to simulate the atmospheric effects of wind turbines off the coast of California, with the goal of providing forcing fields for an ocean circulation model. The WRF-WFP model used two levels of horizontal discretization (Table 1), with each model grid setup using a Mercator projection. The coarse, outer nest consisted of 150 x 144 cells in the latitudinal and longitudinal directions, respectively, with latitudinal spacing that varied from 0.12° to 0.15°, and a longitudinal spacing equal to 0.17° (nominal $\Delta x = 15$ km). The inner, finer nest consisted of 426 x 516 cells, with latitudinal spacing that varied from 0.026° to 0.03°, and a longitudinal spacing equal to 0.035° (nominal $\Delta x = 3$ km). Each nest had 61 terrain-following vertical levels from the sea surface to approximately 20 km height above the sea surface. The horizontal discretization values for each nest correspond to the discretization of an accompanying ocean circulation model and followed recommendations (Tomaszewski and Lundquist 2020) for refinement levels of inner nest WRF-WFP wind-turbine simulations. The extent of the outer (inner) model domain

overlapped with the outer (inner) domain of the accompanying ocean circulation model, while the larger size prevented boundary artifacts arising from the mismatch between boundary conditions and the model solution near the lateral boundaries, which could propagate into the interior of the domain consisting of the wind-energy areas of interest. Both outer and inner domains were centered nominally at the latitude and longitude coordinates of 39°N and 122.75°W, with the outer domain spanning longitudinal values from 136°W to 110°W, and latitudinal values from 29.5°N to 48.5°N. The inner, refined domain spanned longitudinal values from 130°W to 115°W, and latitudinal values from 31.1°N to 45.25°N. Figure 3 shows the model grid extents, topography, and a vertical section of the modeled wind turbines, overlaid on a subset of offshore terrain-following WRF-WFP vertical levels between the surface and 1,200 m above the sea surface (to better highlight vertical discretization around the turbine).

Table 1: WRF-WFP Atmospheric Model Parameters

Parameter:	Value
Resolution:	15 km outer, 3 km inner
Outer Domain Extents:	136°W to 110°W, 29.5°N to 48.5°N
Inner Domain Extents:	130°W to 115°W, 31.1°N to 45.25°N
Number of Cells:	150x144 cells (outer), 426x 516 cells (inner)
Time Step:	1 hour
Number of Vertical Levels:	32
Years Run:	1988-2012

Source: Integral Consulting, Inc.

Model physics parameters and forcing fields used in the WRF-WFP model were identical to the validated model used to develop the Wind Integration National Dataset (WIND) Toolkit (Optis et al., 2020), so no duplicate validation effort was performed for this study. Validation of the WRF-WFP model that formed the basis of the WIND Toolkit consisted of a comparison of hourly and diurnal wind-field predictions to those measured by offshore buoys and coastal radar stations. Raghukumar et al., (2022) contains a detailed description of numerical schemes, physics parameters, and forcing fields.

Figure 3: Atmospheric Model Parameters
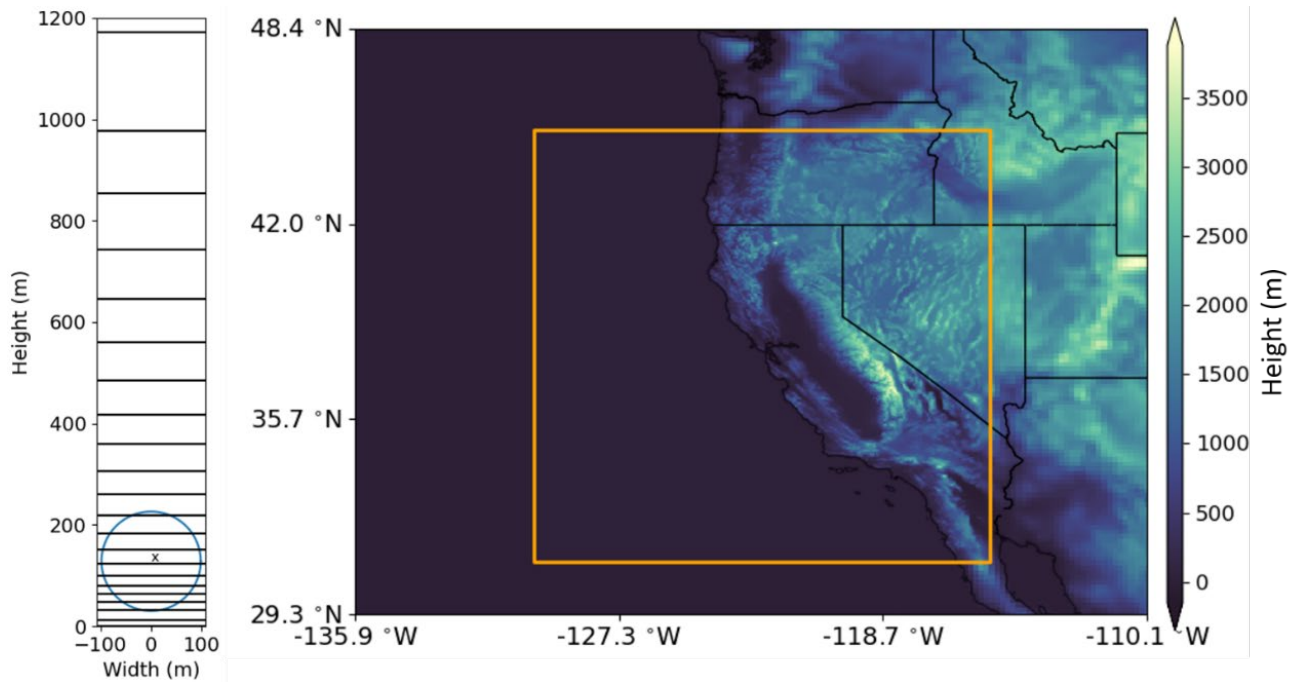
**Atmospheric model turbine hub height and rotor diameter (left),
and WRF-WFP model grid extent and topography (right)**

Source: Integral Consulting, Inc.

Each simulation was performed twice: once without turbines (baseline case) and once with turbines present, every 1 hour for a 25-year period from 1988 to 2012. This period overlapped with boundary conditions for an ocean circulation model, for which the WRF-WFP model output served as forcing fields.

Modeled Wind Turbine Areas of Interest

The primary areas modeled in this study included 10-MW turbines, located within the Humboldt, Morro Bay 399, and Diablo Canyon areas of interest (Figure 4). Additional sensitivity analyses explored implications of 10-MW wind-turbine development in the Humboldt and Morro Bay 376 wind-energy areas, and 15-MW turbine development in the Del Norte, Humboldt, Cape Mendocino, and Morro Bay 376 areas of interest. The primary difference between the Morro Bay 399 and Morro Bay 376 areas of interest is a reduced size in the southeast corner of Morro Bay 376, relative to Morro Bay 399. The last buildout scenario was designed to explore the effects of 20 GW of offshore wind energy, which California's Governor requested as a minimum planning goal for 2045. The CEC adopted a planning goal of 25 GW (Flint et al., 2022) after this buildout scenario was run. Water depths for the turbine locations range from 800 m to 2,000 m, and the simulated wind farms are located 30-50 km offshore.

Figure 4: Modeled Wind Energy Areas of Interest
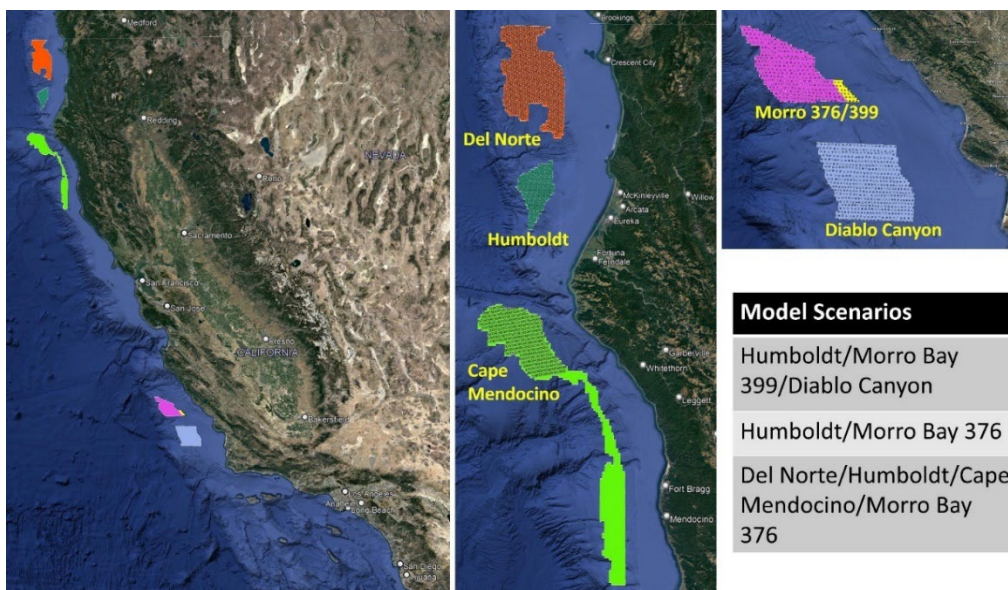
Location of wind energy areas of interest along the California coast (left), and modeled layouts of turbines within the Del Norte, Humboldt, and Cape Mendocino (middle), and Morro Bay and Diablo Canyon areas of interest (right)

Source: Integral Consulting Inc.

Turbine Parameters

Turbine parameters were from the 10-MW and 15-MW floating offshore turbine models (Beiter et al., 2020), with commercial operation dates of 2022 and 2030, respectively. Turbines were placed within each wind-energy area of interest and assumed a full project build-out, as shown in Figure 4. The locations of turbines within the Humboldt wind energy area of interest were identical to those previously reported (Severy et al., 2020), and consisted of 152 turbines spaced roughly 1.8 km apart. Similar 9-turbine-diameter spacing was applied to the Morro Bay 399 and Diablo Canyon wind energy areas of interest, resulting in a total of 230 and 495 turbines in each Central Coast wind energy area of interest, respectively, for a grand total of 877 turbines across the three areas, shown in Table 2.

Table 2: Turbine Parameters

| Parameter:	Value
Number of Turbines:	567 (Del Norte), 152 (Humboldt), 297 (Cape Mendocino), 230 (Morro Bay 399), 318 (Morro Bay 376), 495 (Diablo Canyon)
Hub Height:	128 m (10 MW turbine), 150 m (15 MW turbine)
Rotor Diameter:	196 m (10 MW turbine), 240 m (15 MW turbine)
Power Output:	10 MW (Humboldt, Morro Bay 399/376, Diablo run), 15 MW (Del Norte, Cape Mendocino, Humboldt, Morro Bay 376 run)
Turbine Spacing:	1.8 km (~9D)

Source: Integral Consulting, Inc.

Ocean Circulation Model

The study used the ROMS ocean circulation model (Shchepetkin and McWilliams, 2003), with the parameters shown in Table 3. ROMS is a free-surface, terrain-following, primitive equations ocean model widely used by the scientific community for a diverse range of applications (Haidvogel et al., 2000, Marchesiello et al., 2003, Peliz et al, 2003, Di Lorenzo 2003, Dinniman et al., 2003, Budgell 2005, Wilkin et al., 2005). The model consisted of two domains, shown in Figure 5: the outer domain (referred to as WC12), spanning the middle of the Baja Peninsula to the southern tip of Vancouver Island and over 1,000 km zonally, covering 30°N to 48°N and 115.5°S to 134°W at 10 km resolution (with 42 terrain-following vertical levels), and the inner domain or nest (referred to as WC15) spanning from 32°N to 44°N and 116°W to 128°W at 3 km resolution, also with 42 terrain-following vertical levels. Surface forcing fields consisted of WRF-WFP (Raghukumar et al., 2022) horizontal wind speeds 10 m above the sea surface, air temperature, and specific humidity 2 m above the sea surface, surface air pressure, precipitation, downward longwave radiation, and net shortwave radiation. The surface forcing fields for the WC12/WC15 domains consisted of WRF-WFP fields from the outer and inner WRF-WFP domains, linearly interpolated onto the ROMS domains. Boundary and initial conditions for the WC12 model were from a data assimilative reanalysis of a previous version of the WC12 model (Neveu et al., 2016, https://oceanmodeling.ucsc.edu/index.html), which in turn was initialized by the Simple Ocean Data Assimilation (SODA) analysis of the global upper ocean (Carton et al., 2000).

The ocean model was run over the 25-year period of 1988-2012. This long duration was necessary to capture both El Niño and La Niña cycles and distinguish wind farm-induced changes from eddy variabilities.

Figure 5: Ocean Circulation Model Bathymetry
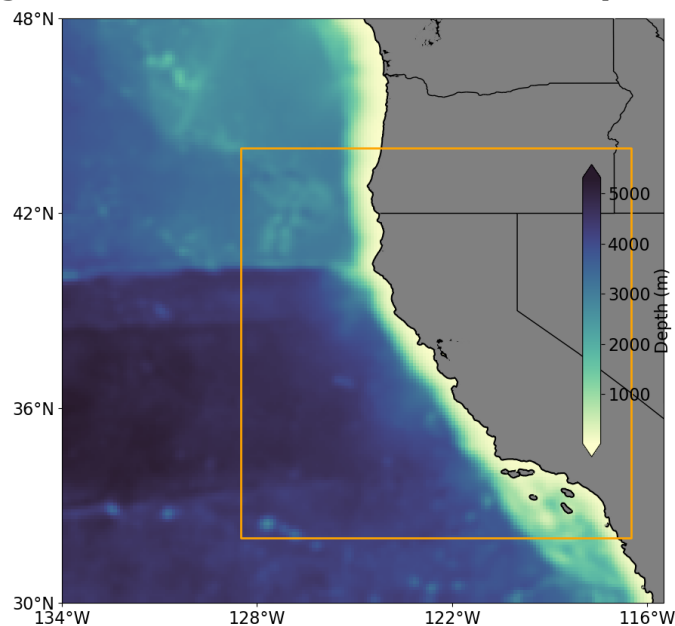
ROMS ocean circulation model bathymetry for each domain: the 10 km outer domain (WC12, full extent of the map) and the 3 km inner domain (WC15), demarcated by the orange box.

Source: Integral Consulting, Inc.

The effects of wind turbines on ocean circulation were modeled through changes in the atmospheric forcing fields, primarily from wind stress. In particular, there is no interaction of ocean currents with physical turbine structures so there are no mixing or drag effects of currents interacting with turbines accounted for here (Schultze et al., 2020, Dorrell et al., 2022).

Both ROMS models have been used extensively in physical oceanographic and ecosystem studies of the CCS, in addition to forming the basis of operational modeling at the Central California Ocean Observing System. The validated WC12 model (Veneziani et al., 2009) was coupled with a lower-trophic-level ecosystem model (Goebel et al., 2010, Fiechter et al., 2018, Raghukumar et al., 2015), and applied to upwelling-specific studies (Jacox et al., 2015) to look at upwelling variabilities (using historical analysis of circulation of the CCS) and examine canyon-driven nearshore upwelling and its effects on larval transport (Lowe, 2020).

Table 3: Ocean Circulation Model Parameters

Parameter:	Value
Resolution:	WC12: 10 km, WC15: 3 km
Outer Domain (WC12) Extents:	136°W to 115°W, 30°N to 48°N
Inner Domain (WC15) Extents:	130°W to 115°W, 32°N to 44°N
Number of Cells:	180 x 181 cells (WC12), 357 x 357 cells (WC15)
Time Step:	15 minutes (WC12), 5 minutes (WC15)
Number of Vertical Levels:	42 (WC12 & WC15)
Years Run:	1988-2012
Boundary Conditions:	WC12: Data assimilative reanalysis (Neveu et al., 2016), WC15: daily-averaged WC12 fields along WC15 boundary
Forcing Fields:	10 m winds, 2 m air temperature, 2 m specific humidity, surface air pressure, precipitation, downward longwave radiation, net shortwave radiation,
Forcing Fields Data Source:	Atmospheric model (WRF-WFP)
Bathymetry Data Source:	ETOPO1 (NOAA, 2009)
Initial Conditions:	WC12: data assimilative reanalysis (Neveu et al., 2016), WC15: daily-averaged WC12 fields
Outputs (representative subset):	Daily-averaged 3D fields: temperature, salinity, density, velocity, 2D fields: sea surface height, wind stress, depth-averaged velocities, surface stresses, surface heat and salt fluxes.

Source: Integral Consulting, Inc.

Upwelling Metrics

Upwelling indices (Bakun 1973, 1975) have been used for 50 years to monitor and understand coastal upwelling along the West Coast and its effects on the marine ecosystem, from phyto-

plankton to top predators. These indices were initially computed using coarse resolution atmospheric pressure fields. More recent advances (Jacox et al., 2018) allow more accurate quantifications for both upwelling and downwelling, as well as nutrient fluxes associated with this transport. Specifically, two indices are routinely produced at the National Oceanic and Atmospheric Administration's Southwest Fisheries Science Center: the Coastal Upwelling Transport Index (CUTI), which estimates vertical water volume transport, and the Biologically Effective Upwelling Transport Index (BEUTI), which estimates vertical nitrate flux.

In this study, the CUTI and BEUTI indices were computed based on the high-resolution ocean and atmosphere model outputs previously described.

Both indices were computed in one-degree latitude bins along the West Coast. The cross-shore extent of upwelling captured by the indices can vary, though a cross-shore integration distance of 75 km is typically used to encompass the nearshore region. These indices were also computed in 10-km cross-shore bins to better resolve upwelling changes within 100 km of the coast (wind-energy areas of interest were centered approximately 45 km offshore); CUTI was calculated as the net transport out of a given latitudinal bin, which must be balanced by vertical transport into the surface mixed layer. The vertical nitrate flux (BEUTI) was calculated by multiplying CUTI by the nitrate concentration at the base of the mixed layer. Since the ocean model does not explicitly represent nitrate, it was estimated from a latitude-nitrate-temperature relationship that is very robust in the CCS (capturing 95 percent of the observed nitrate variance, Jacox et al., 2018).

Model Validation

The physics parameters and forcing fields used in the WRF-WFP model implementation were identical to the validated model used to develop the offshore wind resource characterization as part of the WIND Toolkit (Optis et al., 2020). Therefore, no duplicate validation effort was performed for the atmospheric model in this study.

An atmospheric-ocean circulation model evaluation exercise was performed using ocean model output in the absence of turbines. Sea surface temperature (SST) data were obtained over the 1988-2012 period from the NOAA 1/4° Daily Optimum Interpolation Sea Surface Temperature (OISST version 2.1) product. The model-data bias in SST was computed over the WC15 model domain while domain-averaged SSTs were computed along a zone that spanned from the coast to 200 km offshore, between 32-44°N, to focus on model performance within the coastal upwelling region (Figure 6a). The seasonal cycle (the monthly mean climatology) was removed from the domain-averaged SST to focus on the model's ability to accurately capture interannual variability. The model was found to be biased somewhat warm, with a root mean square error (RMSE; computed on the SST anomalies) of 0.4°C. A good model-data correlation ($r^2 = 0.86$) was observed (Figure 6b), showing that the model adequately reproduced regional scale oceanographic processes that drive interannual variability, including warm surface waters during El Niño years (1997-1998) and cooler waters associated with La Niña years (1998-1999).

Figure 6: Ocean Circulation Model Validation
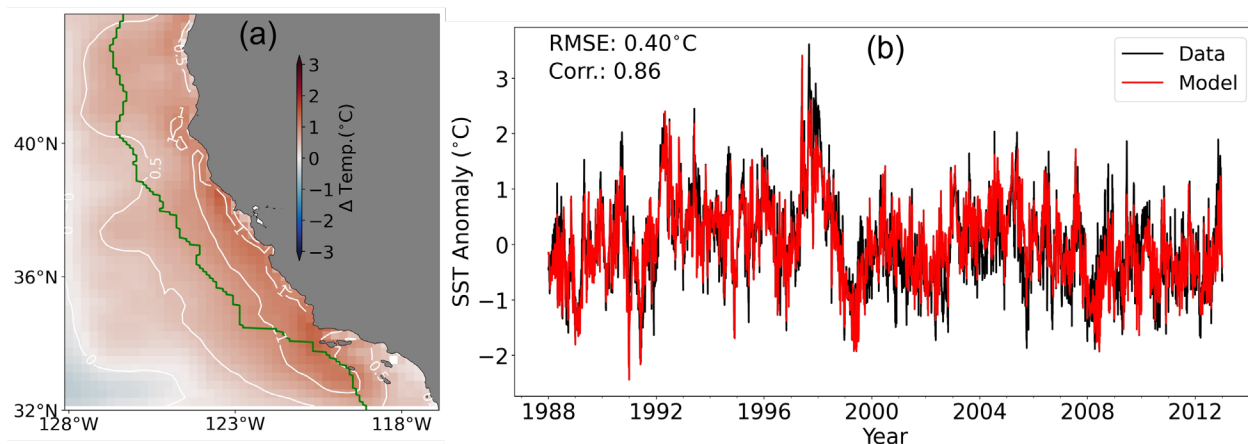
(a) Mean ocean circulation model-data bias in sea surface temperature. White lines indicate 0.5◦C contours, while the green line indicates the boundary of the 0-200 km offshore zone used to compute (b) spatially-averaged sea surface temperatures, relative to the seasonal mean, between 0 and 200 km offshore and 32-44°N, compared to those from the NOAA 1/4° OISST v2.1 product.

Source: Integral Consulting, Inc.

Climate Change Impacts

To place the modeled effects on upwelling within the context of a changing climate, specific years within the 25-year model spanning 1988-2012 were identified as most closely matching changes in winds expected due to climate change in the years 2020-2085. Three climate change scenarios were considered, commonly known as representative concentration pathways (RCP), each of which reflects a different projected emissions scenario.[1] Global maps of wind speeds were downloaded from the Coupled Model Intercomparison Project (CMIP5) effort,[2] which produced projections of atmospheric circulation fields using models from academic and government research groups around the world. Averaged monthly wind fields were obtained at a 2° (2.5°) longitudinal (latitudinal) resolution. The specific model that the fields pertain to is the Geophysical Fluid Dynamics Laboratory's Earth System Model (GFDL-ESM2g).

The global model fields were subsampled within the bounds of the WRF-WFP model, and domain-averaged yearly minima, maxima, and means were computed for the WRF-WFP and climate-change models. WRF-WFP modeled years that most closely aligned with the three sets of climate change projections bookended encapsulated future projections across low- and high-emissions scenarios.

These analyses do not capture all anticipated future changes to the California Current (for example, stratification structure changes from surface heat flux). The analyses represent a first attempt at placing the oceanic changes resulting from offshore wind development in the context of climate change as projected in CMIP5 since CMIP6 data were not yet available.

---

[1] RCP 4.5 is described by the Intergovernmental Panel on Climate Change (IPCC) as a moderate scenario in which emissions peak around 2040 and then decline. RCP 8.5 is the highest baseline emissions scenario (i.e. Business as Usual) in which emissions continue to rise throughout the twenty-first century. In contrast, RCP 2.6 is a very stringent pathway that is likely to keep global temperature rise below 2 °C by 2100.

[2] https://cds.climate.copernicus.eu/cdsapp#!/dataset/projections-cmip5-monthly-single-levels?tab=overview

CHAPTER 3:
Results

Modeled fields are presented in the order of changes to winds (atmospheric circulation), followed by changes to ocean circulation and corresponding changes in upwelling metrics.

Atmospheric Modeling

Longer-term perturbations and changes in wind speed and direction in both the absence and presence of simulated turbines were evaluated for seasonal variability (Figure 7). In this study, the four seasons (winter, spring, summer, and fall) were defined as: January to March, April to June, July to September, and October to December. Sustained northwesterly winds were observed in the spring and summer months; particularly intense winds between 10 and 15 m/s were observed around headlands such as Cape Mendocino, Point Arena and Point Conception (labeled CM, PA and PC, respectively, in Figure 7). Accompanied by the intensification of winds, there were differences in wind speeds at 10 m above sea level that approached 1 m/s (~5 percent reduction) within the Morro Bay and Diablo Canyon areas. Effects observed at the Humboldt site were significantly less than those at the Morro Bay and Diablo Canyon sites, consistent with the smaller area footprint of the Humboldt area of interest.

Figure 7: Seasonal Variability in Modeled Wind Speeds
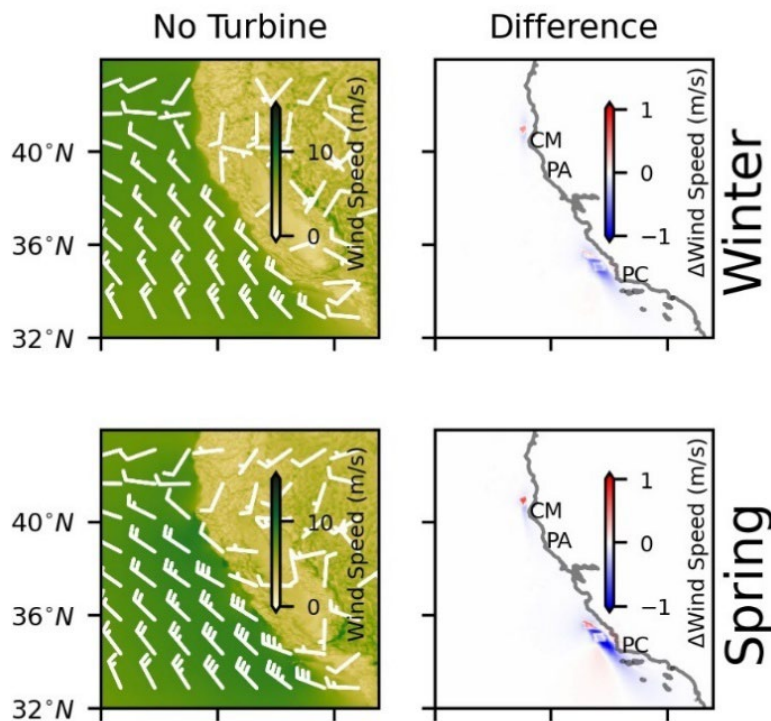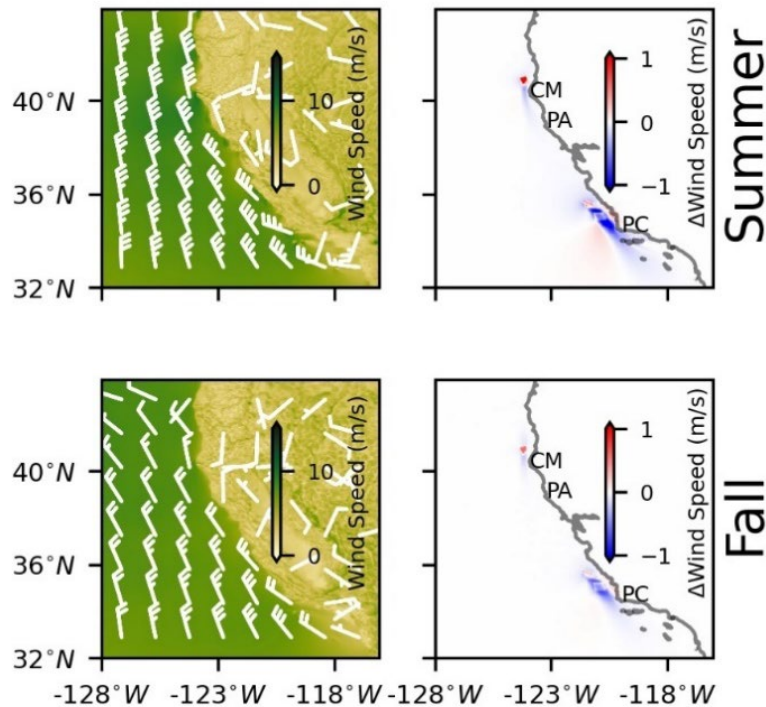
(Left) Seasonal variability in modeled wind speeds 10 m above the sea surface in the absence of turbines, and (right): wind speed differences (baseline minus turbine simulations) for Humboldt, Morro Bay 399, and Diablo Canyon. CM = Cape Mendocino, PA = Point Arena, and PC = Point Conception.

Source: Integral Consulting, Inc.

No measurable change was observed in wind speed directions in the presence of turbines, relative to the baseline condition. As shown in Figure 7, the regional extent of wind speed reduction by wind turbines often extended south past the Channel Islands, covering an area of approximately 12,500 km2, with a length scale of approximately 200 km. Also observed was a seasonal dependence consistent with the fastest wind speeds between April and September. Wind speeds generally trend lower as fall transitions into winter, which is typical of weather patterns along California's coast. Seasonal atmospheric circulation is driven by the North Pacific High and terrestrial surface pressures, which in turn are modulated by seasonal heating and cooling (Huyer 1983).

Other atmospheric fields were also considered: the temperature and relative humidity 2 m above the sea surface, surface pressure, precipitation, and shortwave and net longwave radiation. No significant (relative to baseline) changes in these fields followed the introduction of wind turbines (Raghukumar et al., 2022).

Ocean Modeling

Given that upwelling processes are primarily characterized by vertical transport that transfers cooler, deeper, nutrient-rich waters to surface waters, the contributions of coastal and curl-driven upwelling (and effects of wind turbines on each) are presented first. Each process has vastly different vertical velocities and spatial extents, with different efficacies in delivering nutrients to the euphotic zone. Untangling each process from the ocean model outputs can be

very difficult since curl-driven upwelling can occur in the same zone as coastal upwelling. Separating the two processes is easier using the wind stress fields and assuming that no curl-driven upwelling occurs in a narrow 10 km coastal zone.

Using that assumption, it was found that vertical velocities were generally about twice as strong for coastal upwelling within the narrow 10-km coastal band as for curl-driven upwelling (Figure 8). Vertical velocities near the coast were generally upwelling-favorable during the spring season and accentuated around headlands and topographic features such as Cape Mendocino, Point Arena, and Point Conception (marked as CM, PA and PC in Figure 8) (Dorman et al., 2013). Curl-driven vertical velocities show both upward and downward transport on either side of the wind-energy area of interest. Differences in coastal upwelling from wind-energy extraction were primarily seen as modest reductions in vertical velocity near Point Conception (34°N), and an even smaller reduction near Cape Mendocino. The nearshore side of the simulated wind farm showed a reduction in upwelling, which reinforced the reduction in coastal upwelling near Point Conception, while the offshore side of the simulated wind farm showed enhanced upwelling from Ekman suction.

**Figure 8: Seasonally Averaged Vertical Velocities**
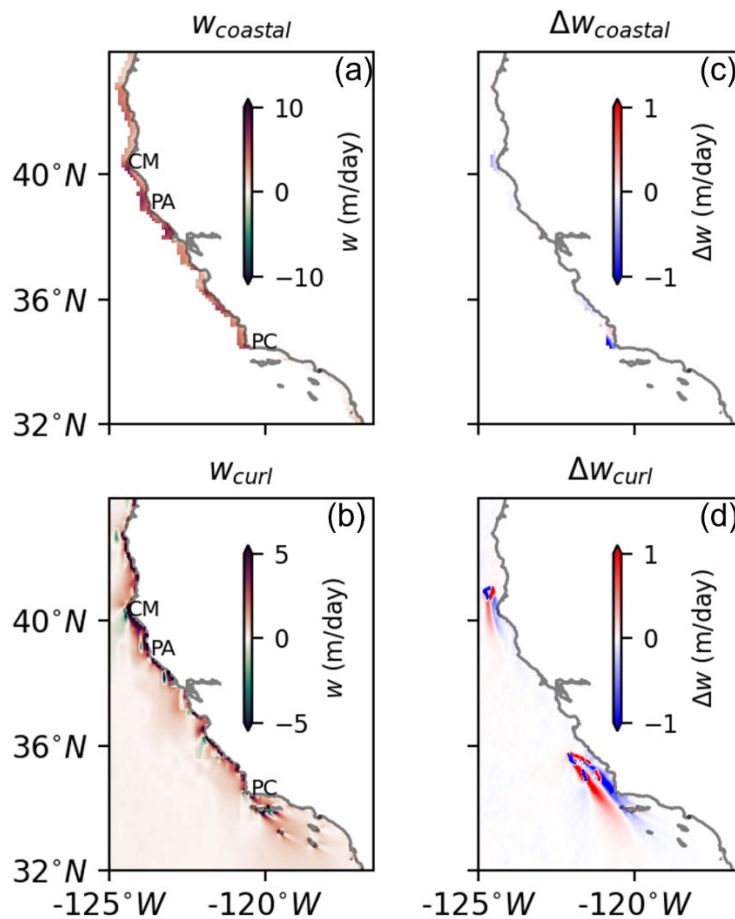
Seasonally averaged vertical velocities during spring for the baseline case, computed from wind fields for (a) coastal and (b) curl-driven upwelling. Differences in each (turbines minus baseline) shown (c) and (d)

Source: Integral Consulting, Inc.

The model fields, evaluated in terms of two metrics for upwelling volume transport (Coastal Upwelling Transport Index (CUTI) and nutrient flux (Biologically Effective Upwelling Transport Index (BEUTI) (Jacox et al., 2018), exhibited similar seasonal and spatial variability, indicating that for the mean patterns, vertical nitrate flux (estimated from a temperature-nitrate relationship) closely tracked upwelling strength. Comparing upwelling indices in the absence of turbines, with the wind field altered by turbines (Figure 9), a reduction in upwelling transport was observed inshore of the simulated wind farms, along with an increase in upwelling offshore of the windfarm areas. The changes in upwelling were primarily outside the 10-km coastal zone, which is usually the region of strongest upwelling (Pickett and Paduan 2003). Similar to changes in wind speed (Figure 7), changes in upwelling were more pronounced at Morro Bay and Diablo Canyon than they would be at Humboldt, likely due to the relatively smaller footprint over which turbines were simulated at Humboldt.

Figure 9: Interannual Mean of CUTI
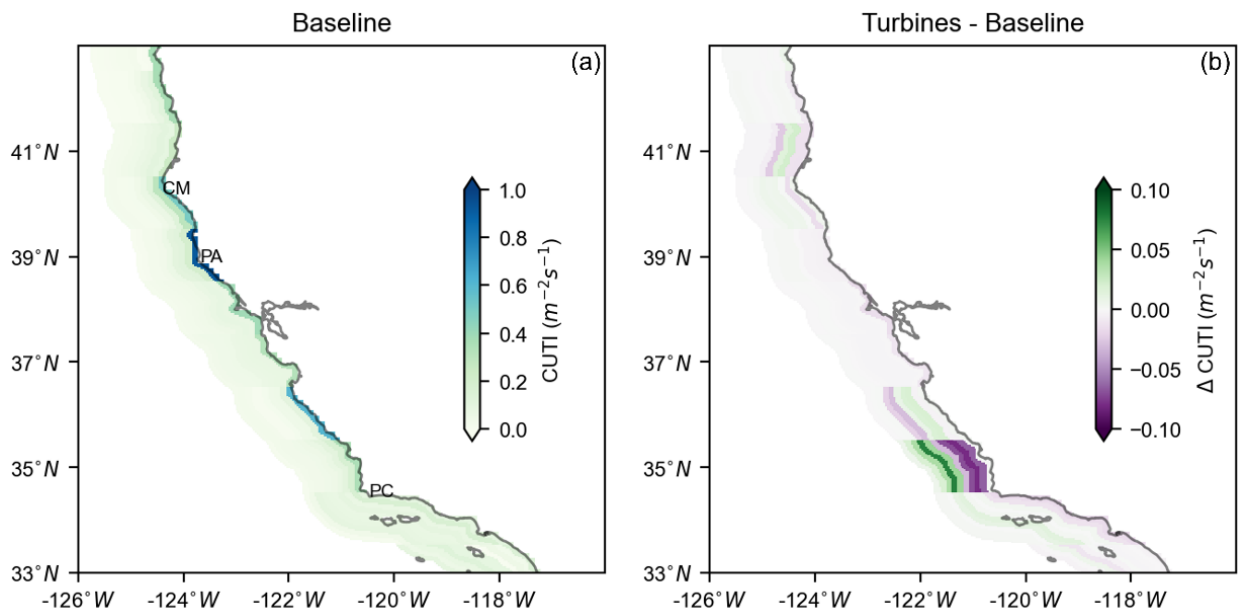
Interannual mean of CUTI (indicating strength of upwelling) for the baseline (left) and differences with turbines (turbines minus baseline; right). CUTI shows a decrease in upwelling with the presence of turbines particularly nearshore (dark purple) and an increase offshore (green) at 35°N

Source: Integral Consulting, Inc.

There was considerable variability in CUTI and BEUTI at 35°N, computed over a 100-km zone along a transect running through the Morro Bay/Diablo Canyon area (Figure 10), which is the region of greatest upwelling change. Of particular note are years when upwelling was either strongly inhibited by El Niño (1991 and 1997) or enhanced by La Niña events (1999 and 2008); BEUTI more closely tracks the baseline case with occasional years (1991, 2001/2002) when BEUTI was either decreased or enhanced more than CUTI. This indicates that wind turbines at 35°N change not only upwelling strength, but also change the subsurface temperatures of upwelled waters, and, by proxy, nitrate concentrations in upwelled waters. The magnitude of mean change in BEUTI and CUTI was sensitive to the cross-shore distance used to calculate net upwelling (Figure 11).

Figure 10: CUTI and BEUTI at 35°N
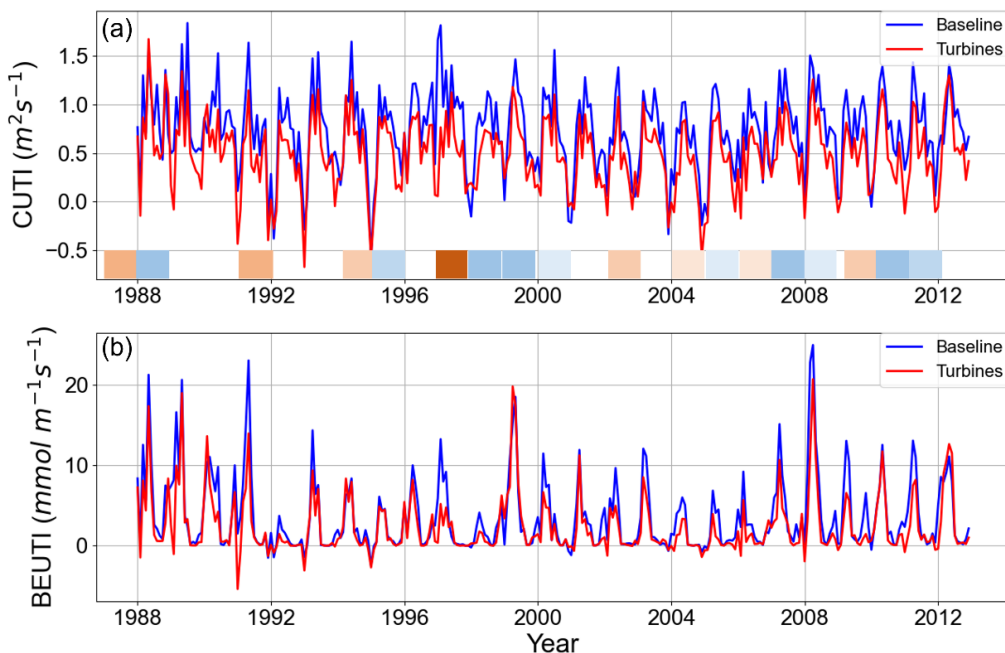
(Top) CUTI and (bottom) BEUTI at 35°N as a function of time, calculated from ocean circulation model fields over a 100-km zone. Weak, moderate, and strong El Niño (orange) and La Niña (blue) periods are shown in the top panel.

Source: Integral Consulting, Inc.

Figure 11: Differences in CUTI and BEUTI
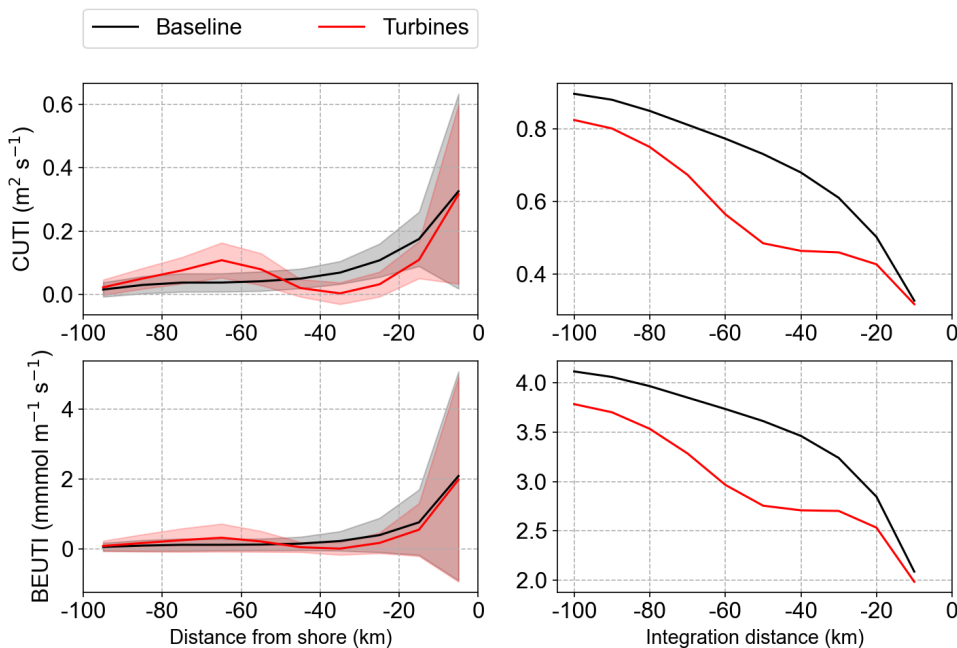
Differences in CUTI (top row) and BEUTI (bottom row) as a function of distance from shore (left) and cross-shore integration distance (right) at 35°N, calculated from ocean circulation model fields over a 100-km zone. Shading indicates the interannual variability (the standard deviation calculated across all years).

Source: Integral Consulting, Inc.

Upwelling at 35°N decreases in an approximately 50-km nearshore zone, offset by increases in upwelling farther offshore. The maximum decrease in integrated upwelling transport and nutrient flux occurred 50 km from the coast (approximately in the center of the simulated windfarm), after which curl-driven increases helped offset upwelling reductions. Changes in CUTI and BEUTI were similar; little to no change was observed in the 10-km zone adjacent to the coast, and the greatest reductions occurred in the 10-50-km zone. The shading in Figure 11 reflects the significant interannual variability seen in CUTI and BEUTI (Figure 10). Over a 100-km integration zone, an analysis of changes (figure not shown) in CUTI and BEUTI exceeded the standard deviation of CUTI and BEUTI just 1.43 percent and 3.21 percent of the time, respectively. However, in specific cross-shore regions (for example, 20-40 km and 60-80 km offshore), turbine-induced upwelling changes can be well outside natural variability (Figure 11, upper left). Subsurface temperatures along a transect at 35°N show modest warming inshore of 50 km once simulated turbines were introduced in the environment, indicating reduced upwelling in this zone (Figure 12). This warming was accompanied by the cooling of subsurface waters offshore of 50 km indicating enhanced upwelling and increased nutrient concentrations in these offshore waters.

Figure 12: Subsurface Temperature at 35°N
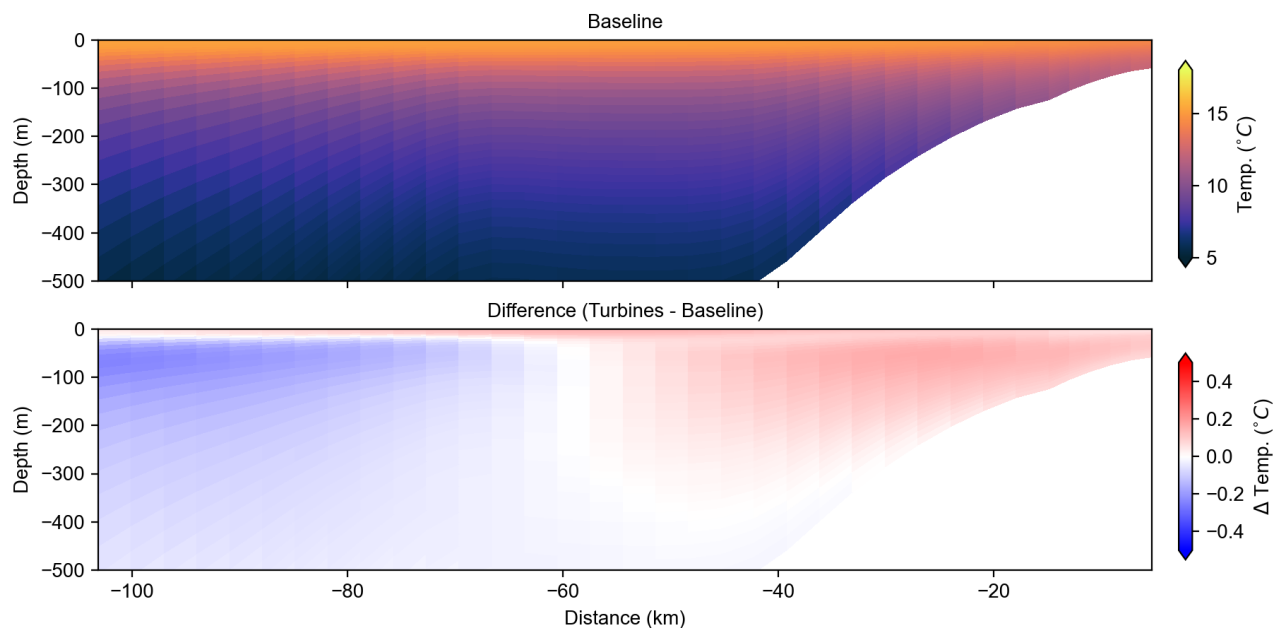
Modeled subsurface temperature at 35°N, as a function of depth and distance to shore for (top) baseline conditions and (bottom) differences from baseline (turbines minus baseline)

Source: Integral Consulting, Inc.

Climate Change Impacts

Specific years where domain-averaged modeled wind speeds, bracketing those predicted by climate change models, are identified in Table 4 for various RCP emissions scenarios from CMIP5 global climate models. For the three scenarios, the minimum and mean wind speeds modeled in the year 1989 most closely matched the minimum and mean wind speeds projected for the future for RCP 2.6, RCP 4.5 and RCP 8.5. Maximum wind speeds for the

California coast under RCP 2.6 and 8.5 occurred historically in 1988, while those under RCP 4.5 occurred in 1989.

Table 4: Climate Change Model Years

	RCP 2.6 - Year	RCP 2.6 - Speed	Corresponding WRF Model - Year	Corresponding WRF Model - Speed	Bias (WRF − RCP)
Min	2075	5.24	1989	5.68	0.47
Max	2021	5.85	1988	5.86	0.01
Mean	2027	5.55	1989	5.68	0.13
	RCP 4.5 - Year	RCP 4.5 - Speed	Corresponding WRF Model - Year	Corresponding WRF Model - Speed	Bias (WRF − RCP)
Min	2036	5.29	1989	5.68	0.39
Max	2054	5.9	1994	5.91	0.00
Mean	2047	5.56	1989	5.68	0.12
	RCP 8.5 - Year	RCP 8.5 - Speed	Corresponding WRF Model - Year	Corresponding WRF Model - Speed	Bias (WRF − RCP)
Min	2045	5.14	1989	5.68	0.54
Max	2024	5.86	1988	5.86	0.00
Mean	2066	5.53	1989	5.68	0.15

Identification of WRF model years where domain-averaged wind speeds most closely matched those from climate change predictions for various projections.

Source: Integral Consulting, Inc.

The years of maximum wind speeds (Figure 13, Figure 14) have an additional peak in CUTI in November, which was not the case in the minimum/mean wind-speed year. The higher wind-speed year also experienced the strongest upwelling event earlier in the year (May as opposed to July for the minimum/mean wind-speed year). Changes in CUTI once turbines were intro-duced appeared to be more pronounced for the lower wind-speed year and more sustained over the course of the year. Changes in BEUTI also appeared larger for the minimum/mean wind speed year leading to the upwelling peak in nutrient flux in May. This analysis was limited to two years in the modeled period (1988 and 1989), which bracketed the minimum, maxi-mum, and mean wind speeds projected over the years 2030-2100, so cannot be considered statistically significant. Nevertheless, this limited analysis appears to show that changes in upwelling from offshore wind-energy development could potentially be reduced in the face of intensifying winds due to climate change.

Figure 13: Climate Change Study Results
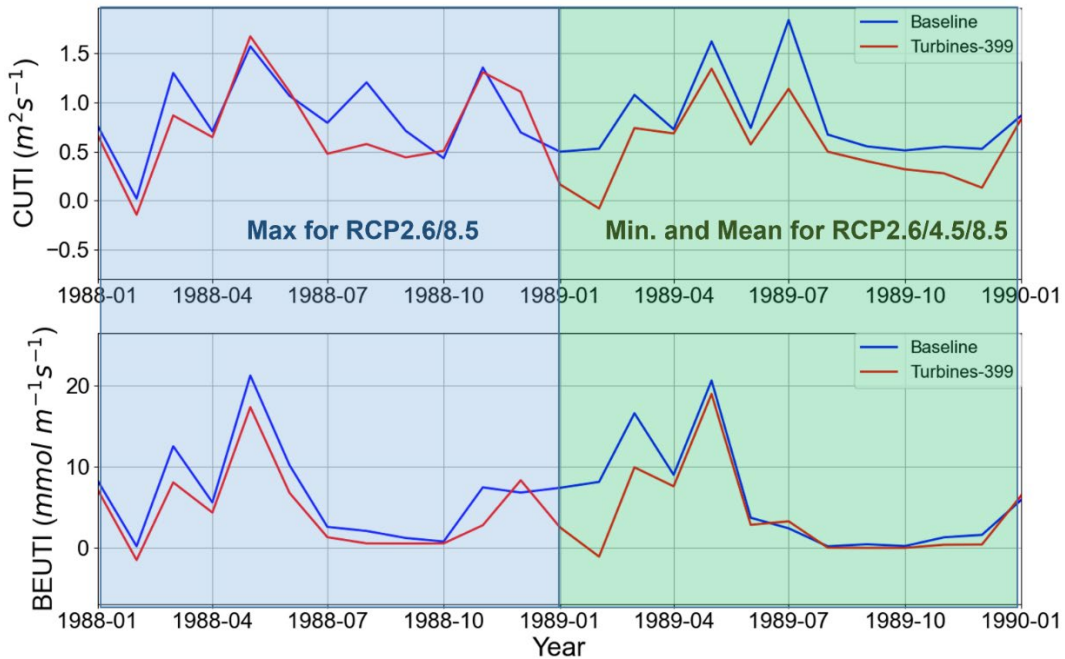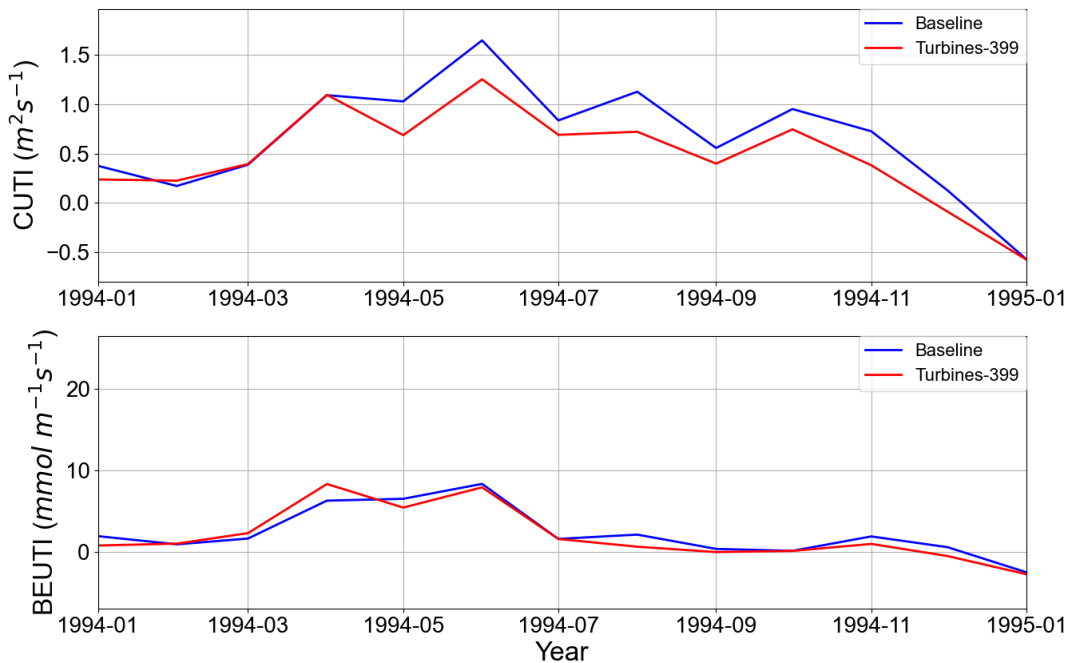

CUTI and BEUTI at 35°N for modeled years that match maximum wind speeds under RCP 2.6/8.5 (blue-1988) and, minimum and mean wind speeds under RCP 2.6/4.5/8.5 (green-1989).

Source: Integral Consulting, Inc.

Figure 14: Maximum Wind Speed Model Results

CUTI and BEUTI for modeled year 1994 that match maximum wind speeds under RCP 4.5

Source: Integral Consulting, Inc.

While it is difficult to draw direct comparisons between baseline results shown in Figure 13 with projected changes in nutrient flux (Xiu et al., 2018), there are some qualitative similarities. For example, the annual mean/max CUTI (upwelling strength index) at 35°N for RCP 8.5 is larger than the mean values shown in Figure 9. This increase is qualitatively consistent with the increase shown in Figure 3 (Xiu et al., 2018).

It is important to consider the effects of offshore windfarms on upwelling circulation in the face of the earth's rapidly changing climate. There have been robust discussions about climate change impacts to upwelling circulation starting with Bakun et al., (1990), who suggested that global warming can result in more intense upwelling from stronger alongshore winds induced by greater land-sea air temperature differences and sharper sea-level pressure gradients. While large-scale empirical evidence (or predictions from ensemble models) of Bakun's hypothesis is yet to be identified, there is increasing evidence to suggest that poleward intensification of upwelling, which along the California coast consists of the region north of 35°N (Sydeman et al., 2014, Rykaczewski et al., 2015). This region encompasses the wind-energy areas of interest considered in this study. Increased oceanic heat content can also increase stratification, however, reducing the source depth of upwelled waters and inhibiting productivity (Jacox et al., 2015). Finally, basin-scale changes in circulation may alter the nutrient content of upwelling source waters, impacting productivity independent of local changes in winds or stratification (Rykaczewski and Dunne, 2010). The interplay of these sometimes competing effects will determine future changes in primary productivity off the California Coast, and climate models do not agree on expected signs of change (Bograd et al., 2023). The environmental effects of wind farms should therefore be considered in the context of future changes. For example, the reduction of upwelling in the 10-50-km cross-shore zone could potentially offset an increase in upwelling from intensification of alongshore winds, while an increase in upwelling further offshore could reinforce climate change-induced changes. Further, two regions of reduced upwelling from windfarms can reinforce reductions (due to increased stratification of the upper ocean), while the region of increased upwelling (cooler water) can offset reductions in upwelling from enhanced stratification. The complex interplay of these processes urgently deserves further examination.

Sensitivity Studies

Additional sensitivity studies were conducted for two scenarios representing both the short-term plans for offshore wind energy development and a longer-term trajectory.

- **Scenario 1** (short-term plans): Buildout of the Humboldt/Morro Bay 376 wind energy areas with 10-MW turbines: the geographical area modeled represents the areas auctioned for lease by BOEM in December 2022.

- **Scenario 2** (long-term trajectory): Buildout of the Del Norte/Humboldt/Cape Mendocino/Morro Bay 376 areas with 15-MW turbines. This is a potential future scenario to achieve a 10-GW buildout as projected in California's *SB 100 Joint Agency Report* (CEC, CPUC, and CARB 2021).

Changes in CUTI for Scenario 1 (Figure 15, left) show smaller changes near the Morro Bay 376 region due to two things: the somewhat smaller geographical coverage of the Morro Bay 376

area relative to Morro Bay 399 (Figure 9), and the exclusion of the Diablo Canyon area of interest. The inshore extent of upwelling reduction was smaller for Morro Bay 376 when compared with the Morro Bay 399 area of interest, while the offshore region of enhanced upwelling appeared to be unchanged in both width and magnitude. Changes near the Humboldt area were identical to those seen in Figure 9 since turbine development remained unchanged in the two simulations.

Figure 15: Changes in CUTI
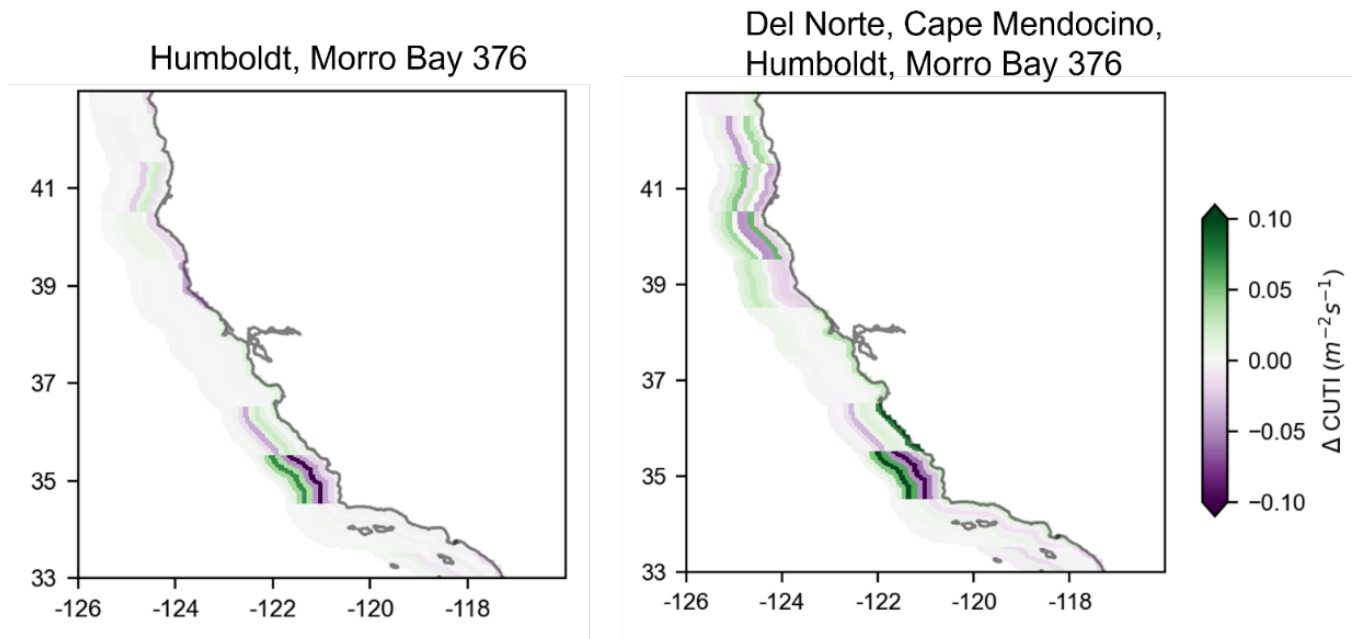
Changes in interannual mean of CUTI (turbines minus baseline) for the Humboldt and Morro Bay 376 areas of interest (Scenario 1, left), and Del Norte, Humboldt, Cape Mendocino and Morro Bay 376 areas of interest (Scenario 2, right)

Source: Integral Consulting, Inc.

Changes in CUTI in Scenario 2 (Figure 15, right) show substantial modifications to upwelling structure near the simulated North Coast turbine areas. The larger north-south area simulations (including the Del Norte, Humboldt, and Cape Mendocino areas of interest) resulted in multiple dipole-like changes in upwelling along the North Coast. Reductions in upwelling in bands along each of these dipoles appear to be mostly balanced by adjacent bands of increases. Changes in upwelling structure near the Morro Bay 376 area (using 15-MW turbines) were more pronounced than in Scenario 1, which used 10-MW turbines. While the cross-shore extent of reductions near Morro Bay 376 was identical using both turbine sizes, the magnitude of changes in upwelling (reductions and increases) was higher. Additionally, the use of higher-capacity turbines caused a coastal band of enhanced upwelling north of the area of interest, which was similar in structure to that observed in Figure 9.

Cross-shore changes in CUTI and BEUTI at 35°N from the 15-MW turbines were compared against the baseline case (no turbines) and the previously studied Morro Bay 399/Diablo Canyon case (Figure 16). Changes to CUTI and BEUTI for the 15-MW Morro Bay 376 case were also more pronounced, both in terms of reductions and increases in upwelling as a

function of distance to shore (Figure 16), and were driven by larger wind curl due to greater energy extraction (and therefore greater shear in wind speed). Integrated changes to the CUTI index (Figure 16, upper right) tended to fall between the baseline and Morro Bay 399 buildout scenarios. Interestingly, the integrated changes in BEUTI show a slight increase over the baseline upwelled nutrient flux at both short (<20 km) and longer (>80 km) integration distances. This increase was due to the presence of cooler subsurface waters (relative to baseline and the Morro Bay 399 scenarios). Since BEUTI is obtained from the inverse relationship between temperature and nitrate concentration, cooler waters resulted in an increase in the BEUTI index.

Figure 16: CUTI and BEUTI for Morro Bay 376
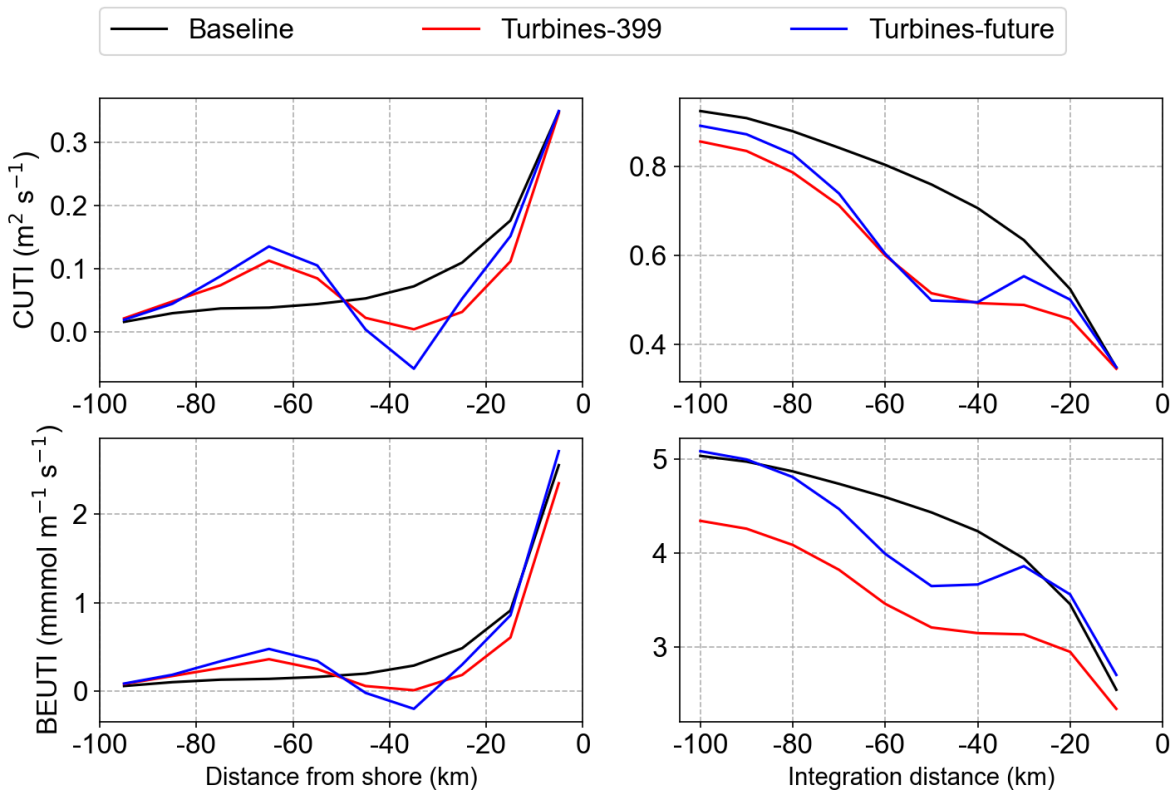
Differences in CUTI (top row) and BEUTI (bottom row) as a function of distance from shore (left) and cross-shore integration distance (right) at 35°N, calculated from ocean circulation model fields over a 100 km zone. The 'turbines-future' curves represent changes due to 15-MW turbines in the Morro Bay 376 area of interest.

Source: Integral Consulting, Inc.

At 40°N, there was little to no change in CUTI or BEUTI from the smaller-sized Humboldt area of interest, but noticeable changes were observed once the four areas of interest were built up with 15-MW turbines (Figure 17). While integrated changes to the CUTI index were minimal, there was a clear increase in BEUTI for nearly all of the integration distances considered (Figure 17, lower right). In this scenario, the increase in BEUTI is also from the presence of cooler waters near the surface.
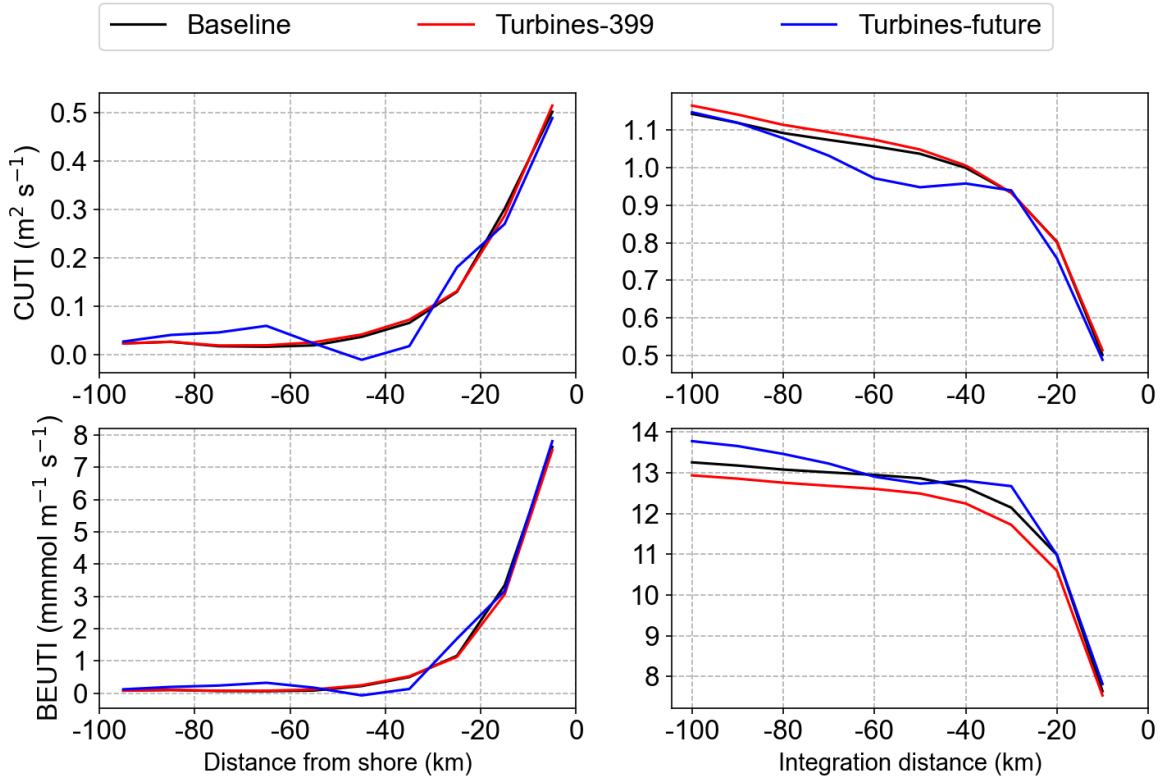
Figure 17: CUTI and BEUTI for Humboldt

Differences in CUTI (top row) and BEUTI (bottom row) at 40°N as a function of distance from shore (left) and cross-shore integration distance (right), calculated from ocean circulation model fields over a 100 km zone. The 'Turbines-future' curves represent changes due to 15 MW turbines in the Humboldt Wind Energy Area and the addition of the Del Norte and Cape Mendocino areas of interest.

Source: Integral Consulting, Inc.

CHAPTER 4:
Conclusion

Upwelling is a dominant driver of ecosystem productivity and variability in eastern boundary currents including the California Current System, which runs along the United States West Coast. Given the importance of upwelling in these regions, estimated indices of upwelling strength are critical for understanding fluctuations in ecosystem properties, ranging from temperature and density to distributions and abundances of top predators. Predictions of upwelling metrics, under a spectrum of environmental conditions and wind farm scenarios, would enable the design and management of the least environmentally impactful offshore wind farm configurations.

The effects of California offshore wind turbines on both the wind stress field and upwelling circulation were studied for baseline (without wind turbines) and modified (simulated wind turbines) scenarios, using atmosphere and ocean circulation models. Model parameters were adjusted to assess sensitive environmental variables and consider hypothetical numbers, locations, and configurations of wind turbines and arrays. Upwelling index metrics quantified changes in upwelling from offshore wind turbine deployment. When expressed in metrics for upwelling strength and nutrient flux, decreases in upwelling were observed on the nearshore side of the simulated windfarm, which was mostly offset by increases in upwelling on the offshore side of the windfarm, suggesting that perhaps there would be an offshore shift in upwelling. Pronounced cross-shore changes to upwelling were observed above levels of natural variability, while indicating more modest changes to total upwelling integrated over a cross-shore transect. The consequences of these changes in the physical upwelling structure on the ecosystem are currently unknown and should potentially direct future areas of investigation, including effects on fisheries and other socioeconomic factors.

The results of this effort will help define policies, facilitate permitting, evaluate the cumulative effects of wind turbine siting, inform construction and operations, clarify tradeoffs, identify data gaps, prioritize research, and expedite device deployment. These outcomes would increase renewable energy generation in California and further diversify the state's clean energy portfolio. Informed projections of upwelling effects of offshore wind development in a modeling framework enable the prioritization and evaluation of mitigation and monitoring needs, which will in turn result in expedited permitting processes and cost reductions for developers and, ultimately, for California's utility ratepayers. This study could easily be extended to evaluate other offshore wind areas of interest in the California Current, including in even deeper waters and with other turbine and layout designs.

Results from this modeling study will hopefully motivate a concerted effort to validate or otherwise verify these results with alternate methods such as onsite or satellite measurements. Based on this study's results, recommendations for future efforts include:

- Evaluation of upwelling effects on phytoplankton, zooplankton, krill, and higher trophic-level responses. The accurate inference of ecosystem responses requires the specific

computation of phytoplankton, zooplankton, and trophic level responses to physical driving factors, which were all beyond the scope of this study.

- Use of a formal risk assessment framework to evaluate fisheries and socioeconomic factors.

- Evaluation of near-field effects from physical turbine structures, and their interactions with larger-scale upwelling circulation.

- Use of fully coupled atmospheric and ocean circulation models capable of accounting for two-way momentum exchanges across the air-sea interface.

- Projection of changes to upwelling circulation using new-generation climate projections, such as those provided by the CMIP6 effort.

GLOSSARY AND LIST OF ACRONYMS

Term	Definition
BEUTI	Biologically Effective Upwelling Transport Index
BOEM	Bureau of Ocean Energy Management
CCS	California current system
CUTI	Coastal Upwelling Transport Index
NOAA	National Oceanic and Atmospheric Administration
RCP	representative concentration pathways
ROMS	Regional Oceanic Modeling System
SODA	Simple Ocean Data Assimilation
SST	sea surface temperature
UCSC	University of California Santa Cruz
WFP	wind farm parameterization
WIND	Wind Integration National Dataset
WRF	Weather Research and Forecasting

References

Bakun, A. 1973. Coastal upwelling indices, west coast of North America, 1946-71. NOAA Technical Report NMFS SSRF-671, Seattle, WA.

Bakun, A. 1975. Daily and weekly upwelling indices, west coast of North America, 1967-73. U.S. Department of Commerce, NOAA Tech. Rep., NMFS SSRF-673.

Bakun, A. 1990. Global climate change and intensification of coastal ocean upwelling. Science 247(4939), 198–201.

Beiter, P., Musial, W., Duffy, P., Cooperman, A., Shields, M., Heimiller, D., Optis, M. 2020. The cost of floating offshore wind energy in California between 2019 and 2032. Technical report, National Renewable Energy Laboratory (NREL), Golden, CO (United States).

Bograd, S.J., M.G. Jacox, E.L. Hazen, E. Lovecchio, I. Montes, M. Pozo Buil, L.J. Shannon, W.J. Sydeman, R.R. Rykaczewski. 2023. Climate change impacts on eastern boundary upwelling systems. Annual Review of Marine Science, 15.

Broström, G. 2008. On the influence of large wind farms on the upper ocean circulation. Journal of Marine Systems 74(1-2), 585–591.

Budgell, W. 2005. Numerical simulation of ice-ocean variability in the Barents Sea region. Ocean Dynamics 55(3), 370–387.

Carton, J.A., G. Chepurin, X. Cao. 2000. A simple ocean data assimilation analysis of the global upper ocean 1950–95. Part II: Results. Journal of Physical Oceanography 30(2), 311-326.

CEC, CPUC, and CARB. 2021. 2021 SB 100 Joint Agency Report Achieving 100 Percent Clean Electricity in California: An Initial Assessment. Publication Number: CEC-200-2021, https://efiling.energy.ca.gov/EFiling/GetFile.aspx?tn=237167&DocumentContentId=70349.

Checkley Jr, D.M., Barth, J.A. 2009. Patterns and processes in the California Current System. Progress in Oceanography 83(1-4), 49–64.

Christiansen, N., U. Daewel, B. Djath, C. Schrum. 2022. Emergence of large-scale hydrodynamic structures due to atmospheric offshore wind farm wakes. Frontiers in Marine Science, 64.

Churchfield, M.J., S. Lee, J. Michalakes, P.J. Moriarty. 2012. A numerical study of the effects of atmospheric and wake turbulence on wind turbine dynamics. Journal of turbulence (13), 14.

Collier, R., S. Hull, O. Sawyerr, S. Li, M. Mogadali, D. Mullen, A. Olson. 2019. California Offshore Wind: Workforce Impacts and Grid Integration. Center for Labor Research and Education, University of California, Berkeley. September 2019. http://laborcenter.berkeley.edu/offshore-wind-workforce-grid

Di Lorenzo, E. 2023. Seasonal dynamics of the surface circulation in the Southern California Current System. Deep Sea Research Part II: Topical Studies in Oceanography 50(14-16), 2371–2388.

Dinniman, M.S., J.M. Klinck, W.O. Smith Jr. 2003. Cross-shelf exchange in a model of the Ross Sea circulation and biogeochemistry. Deep Sea Research Part II: Topical Studies in Oceanography 50(22-26), 3103–3120.

Dorman, C.E., J.F. Mejia, D. Koračin. 2013. Impact of US west coastline inhomogeneity and synoptic forcing on winds, wind stress, and wind stress   curl during upwelling season. Journal of Geophysical Research: Oceans 118(9), 4036–4051.

Dorrell, R., C. Lloyd, B. Lincoln, T. Rippeth, J. Taylor, C.-c. Caulfield, J. Sharples, et al. 2021. Anthropogenic Mixing of Seasonally Stratified Shelf Seas by Offshore Wind Farm Infrastructure. Frontiers in Marine Science, 22.

Duin, M. 2019. Effect of wind farms at the North Sea on meteorological conditions in the Netherlands. Master's thesis. Wageningen University & Research.

Eriksson, O., J. Lindvall, S.-P. Breton, S. Ivanell. 2015. Wake downstream of the Lillgrund wind farm- a comparison between LES using the actuator disc method and a Wind Farm Parametrization in WRF. In: Journal of Physics: Conference Series, vol. 625, IOP Publishing, p. 012028.

Fiechter, J., C.A. Edwards, A.M. Moore. 2018. Wind, circulation, and topographic effects on alongshore phytoplankton variability in the California Current. Geophysical Research Letters 45(7), 3238–3245.

Flint, S., R. deMesa, P. Doughman, E. Huber. 2022. Offshore Wind Development off the California Coast: Maximum Feasible Capacity and Megawatt Planning Goals for 2030 and 2045. California Energy Commission. Publication Number: CEC-8002022-001-REV.

Floeter, J., T. Pohlmann, A. Harmer, C. Mollmann. 2022. Chasing the offshore wind farm wind-wake-induced upwelling/downwelling dipole. Frontiers in Marine Science 9. https://doi.org/10.3389/fmars.2022.

Goebel, N.L., C.A. Edwards, J.P. Zehr, M.J. Follows. 2010. An emergent community ecosystem model applied to the California Current System. Journal of Marine Systems 83(3-4), 221–241.

Haidvogel, D.B., H.G. Arango, K. Hedstrom, A. Beckmann, P. Malanotte- Rizzoli, A.F. Shchepetkin. 2000. Model evaluation experiments in the North Atlantic Basin: simulations in nonlinear terrain-following coordinates. Dynamics of Atmospheres and Oceans 32(3-4), 239–281.

Huang, H.-Y., A.D. Hall. 2015. Preliminary assessment of offshore wind development impacts on marine atmospheric environment: Final project report. Technical report, UCLA Department of Atmospheric and Oceanic Sciences, Los Angeles, CA.

Jacox, M.G., J. Fiechter, A.M. Moore, C.A. Edwards. 2015. ENSO and the California Current coastal upwelling response. Journal of Geophysical Research: Oceans 120(3), 1691–1702.

Jacox, M.G., C.A. Edwards, E.L. Hazen, S.J. Bograd. 2018. Coastal upwelling revisited: Ekman, Bakun, and improved upwelling indices for the US West Coast. Journal of Geophysical Research: Oceans 123(10), 7332–7350.

Jiménez, P.A., J. Navarro, A.M. Palomares, J. Dudhia, 2015. Mesoscale modeling of offshore wind turbine wakes at the wind farm resolving scale: a composite-based analysis with the Weather Research and Forecasting model over Horns Rev. Wind Energy 18(3), 559–566.

Lee, J.C.Y., J.K. Lundquist. 2017. Evaluation of the wind farm parameterization in the Weather Research and Forecasting model (version 3.8.1) with meteorological and turbine power data. Geoscientific Model Development 10(11), 4229–4244.

Lowe, A.B. 2020. Modeling of coastal processes and Lagrangian transport around the Monterey Peninsula. Ph.D. thesis, University of California Santa Cruz.

Marchesiello, P., J.C. McWilliams, A. Shchepetkin. 2003. Equilibrium structure and dynamics of the Current System. Journal of Physical Oceanography 33(4), 753–783.

Musial, W., P. Beiter, S. Tegen, A. Smith. 2016. Potential offshore wind energy areas in California: An assessment of locations, technology, and costs. Technical report, National Renewable Energy Laboratory (NREL), Golden, CO (United States).

Neveu, E., A.M. Moore, C.A. Edwards, J. Fiechter, P. Drake, W.J. Crawford, M.G. Jacox, E. Nuss. 2016. An historical analysis of the California Current circulation using ROMS 4D-Var: System configuration and diagnostics. Ocean Modelling 99, 133–151.

NMFS-F/SPO-187A, N.T.M. 2018. Fisheries economics of the United States 2016. Economics and sociocultural status and trends series. Technical report, National Oceanic and Atmospheric Administration, National Marine Fisheries Service.

Optis, Michael, Oleksa Rybchuk, Nicola Bodini, Michael Rossol, and Walter Musial. Offshore Wind Resource Assessment for the California Pacific Outer Continental Shelf (2020). No. NREL/TP-5000-77642. National Renewable Energy Lab. (NREL), Golden, CO (United States), 2020Paskyabi, M.B., I. Fer. 2012. Upper ocean response to large wind farm effect in the presence of surface gravity waves. Energy Procedia 24, 245–254.

Paskyabi, M.B. 2015. Offshore wind farm wake effect on stratification and coastal upwelling. Energy Procedia 80, 131–140.

Peliz, Á., J. Dubert, D.B. Haidvogel, B. Le Cann. 2003. Generation and unstable evolution of a density-driven eastern poleward current: The Iberian poleward current. Journal of Geophysical Research: Oceans 108(C8).

Pickett, M.H., J.D. Paduan. 2003. Ekman transport and pumping in the California Current based on the US Navy's high-resolution atmospheric model (COAMPS). Journal of Geophysical Research: Oceans 108(C10).

Raghukumar, K., C.A. Edwards, N.L. Goebel, G. Broquet, M. Veneziani, A.M. Moore, J.P. Zehr. 2015. Impact of assimilating physical oceanographic data on modeled ecosystem dynamics in the California Current System. Progress in Oceanography 138, 546–558.

Raghukumar K, C. Chartrand, G. Chang, L. Cheung, J. Roberts. 2022. Effect of Floating Offshore Wind Turbines on Atmospheric Circulation in California. Frontiers in Energy Research, 660. https://doi.org/10.3389/fenrg.2022.863995

Rykaczewski, R.R., D.M. Checkley. 2008. Influence of ocean winds on the pelagic ecosystem in upwelling regions. Proceedings of the National Academy of Sciences 105(6), 1965–1970.

Rykaczewski, R.R., J.P. Dunne. 2010. Enhanced nutrient supply to the California Current Ecosystem with global warming and increased stratification in an earth system model. Geophysical Research Letters 37(21).

Rykaczewski, R.R., J.P. Dunne, W.J. Sydeman, M. García-Reyes, B.A. Black, S.J. Bograd. 2015. Poleward displacement of coastal upwelling-favorable winds in the ocean's eastern boundary currents through the 21st century. Geophysical Research Letters, 42 (15), 6424-6431.

Severy, M., T. Garcia. 2020. Description of study assumptions. In: Severy, M., Alva, G., Chapman, G., Cheli, M., Garcia, T., Ortega, C., N., S., Younes, A., Zoellick, J., A., J. (eds.) California North Coast Offshore Wind Studies. Humboldt. Schatz Energy Research Center, CA.

Schultze, L.K.P., L.M. Merckelbach, J. Horstmann, S. Raasch, J.R. Carpenter. 2020 Increased mixing and turbulence in the wake of offshore wind farm foundations. Journal of Geophysical Research: Oceans 125(8), e2019JC015858.

Shchepetkin, A., J. McWilliams. 2003. The Regional Ocean Modeling System: A split-explicit, free-surface, topography-following-coordinate oceanic model. Institute of Geophysics and Planetary Physics, University of California, Los Angeles.

Sydeman, W.J., M. García-Reyes, D.S. Schoeman, R.R. Rykaczewski, S.A. Thompson, B.A. Black, S.J. Bograd. 2014. Climate change and wind intensification in coastal upwelling ecosystems. Science, 345(6192), 77-80.

Szoeke, R.D., J. Richman. 1985. On wind-driven mixed layers with strong horizontal gradients—a theory with application to coastal upwelling. Journal of physical oceanography 14(2), 364–377.

Tomaszewski, J.M., J.K. Lundquist. 2020. Simulated wind farm wake sensitivity to configuration choices in the Weather Research and Forecasting model version 3.8.1. Geoscientific Model Development, 13(6), 2645-2662.

Veneziani, M., C. Edwards, J. Doyle, D. Foley. 2009. A central California coastal ocean modeling study: 1. Forward model and the influence of realistic versus climatological forcing. Journal of Geophysical Research: Oceans 114(C4).

Wilkin, J.L., H.G. Arango, D.B. Haidvogel, C.S. Lichtenwalner, S.M. Glenn, K.S. Hedström. 2005. A regional ocean modeling system for the long-term ecosystem observatory. Journal of Geophysical Research: Oceans 110(C6).

Wiser, R., K. Jenni, J. Seel, E. Baker, M. Hand, E. Lantz, A. Smith. 2016. Forecasting wind energy costs and cost drivers: the views of the world's leading experts. LBNL-1005717.

Xiu, P., F. Chai, E.N. Curchitser, F.S. Castruccio. 2018. Future changes in coastal upwelling ecosystems with global warming: The case of the California Current System. Scientific reports 8(1), 1–9.

Project Deliverables

- Atmospheric Model Report

- Ocean Circulation Model Report

- Upwelling Metrics Report